

JANUARY 2019

M.Sc. in Electrical and Electronics Engineering

WALEED AL-JUMAILI

**REPUBLIC OF TURKEY
GAZIANTEP UNIVERSITY
GRADUATE SCHOOL OF
NATURAL & APPLIED SCIENCES**

**ANGLE CONTROL OF A SINGLE-DEGREE-OF-FREEDOM
MECHANICAL HELICOPTER MODEL**

M. Sc. THESIS

IN

ELECTRICAL AND ELECTRONICS ENGINEERING

BY

WALEED AL-JUMAILI

JANUARY 2019

**Angle Control Of A Single-Degree-Of-Freedom Mechanical
Helicopter Model**

M.Sc. Thesis

in

Electrical and Electronics Engineering

Gaziantep University

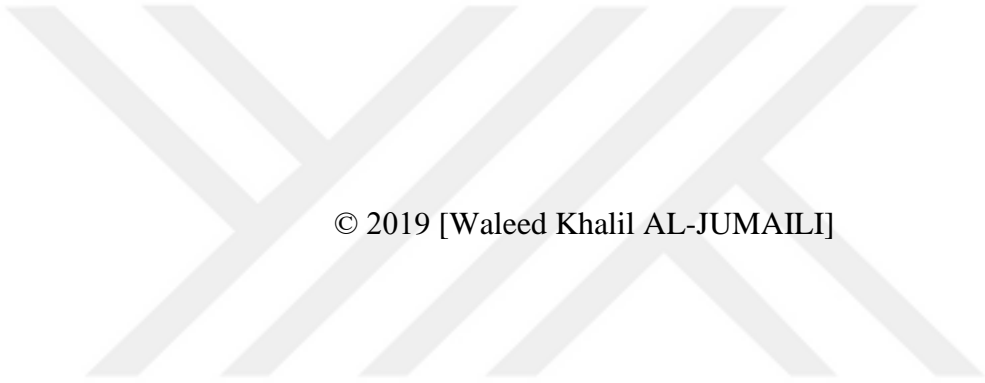
Supervisor

Assist. Prof. Dr. Tolgay KARA

by

Waleed Khalil AL-JUMAILI

JANUARY 2019



© 2019 [Waleed Khalil AL-JUMAILI]

REPUBLIC OF TURKEY
GAZIANTEP UNIVERSITY
GRADUATE SCHOOL OF NATURAL & APPLIED SCIENCES
ELECTRICAL-ELECTRONICS ENGINEERING

Name of the thesis: Angle control of a single-degree-of-freedom mechanical
helicopter model

Name of the student: Waleed Khalil Shehan AL-JUMAILI

Exam date: 31.01.2019

Approval of the Graduate School of Natural and Applied Sciences

Prof.Dr.Ahmet Necmeddin YAZICI

Director

I certify that this thesis satisfies all the requirements as a thesis for the degree of
Master of Science

Prof. Dr. Ergun ERÇELEBİ

Head of Department

This is to certify that we have read this thesis and that in our consensus opinion it is
fully adequate, in scope and quality, as a thesis for the degree of Master of Science.

Assist. Prof. Dr. Tolgay KARA
Supervisor

Examining Committee Members:

Signature

Assoc. Prof. Ahmet Mete VURAL

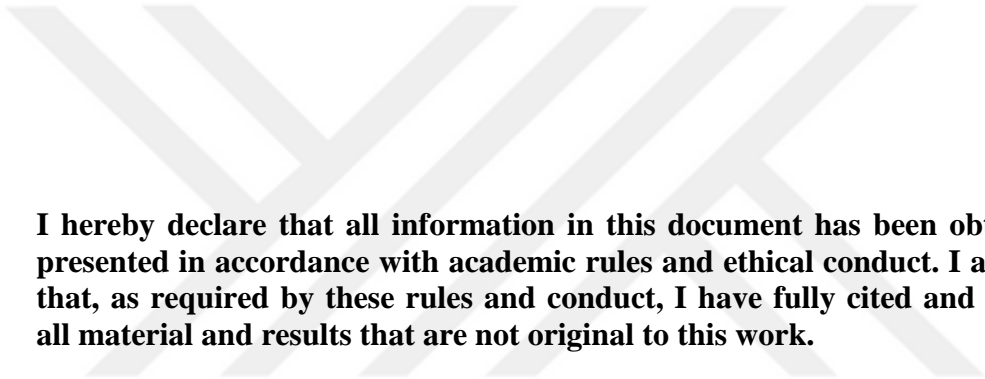
.....

Assist. Prof. Kadir Sercan BAYRAM

.....

Assist. Prof. Tolgay KARA

.....



I hereby declare that all information in this document has been obtained and presented in accordance with academic rules and ethical conduct. I also declare that, as required by these rules and conduct, I have fully cited and referenced all material and results that are not original to this work.

Waleed Khalil Shehan AL-JUMAILI

ABSTRACT

ANGLE CONTROL OF A SINGLE-DEGREE-OF-FREEDOM MECHANICAL HELICOPTER MODEL

AL-JUMAILI Waleed Khalil Shehan

M.Sc. in Electrical and Electronics Engineering

Supervisor: Assist. Prof. Dr. Tolgay KARA

January 2019

48 pages

A helicopter has a lot of uncertainties and disturbances affecting its aerodynamics, which raises the need for robust control. In this thesis a single-degree-of-freedom (1-DOF) laboratory scale helicopter model is designed and controlled via Proportional Integral Derivate (PID) control and Sliding Mode Control (SMC), both of which have solid performances to reject disturbances. The PID and SMC controllers are tested in presence of different types of uncertainties. The helicopter model consists of one arm that rotates on a rigid base with brushless Direct Current (DC) motor driven propeller on one side and counterweight on the other side. Proposed control methodologies are applied to improve the control performance of 1-DOF helicopter model. A potentiometer is used to measure the rotation angle, DAQ-6353 card is used for communication between computer and the Electronic Speed Controller (ESC). The performances are observed in terms of how fast arm angle follows the desired setpoint and also the steady state error. Results show that the desired robustness is obtained using the SMC and the control performance for the SMC is better than the PID.

Keyword: 1-DOF helicopter, PID, SMC, Brushless DC motor.

ÖZET

TEK SERBESTLİK DERECELİ MEKANİK HELİKOPTER MODELİNİN AÇI DENETİMİ

AL-JUMAILI waleed Khalil Shehan

Yüksek Lisans Tezi, Elektrik-Elektronik Mühendisliği

Tez Yöneticisi: Dr.Öğr.Üyesi Tolgay KARA

Ocak 2019

48 sayfa

Bir helikopterin aerodinamiğinde, gürbüz denetimi gerekli kılan çok sayıda belirsizlik ve bozucu etkisi mevcuttur. Bu tezde, tek serbestlik dereceli (1-DOF) laboratuvar boyutunda bir helikopter modeli tasarlanmış ve her ikisi de bozucu etkilerini gidermekte sağlam başarıma sahip olan oransal-integral-türevsel (PID) denetleyici ve kayan kipli denetleyici (SMC) ile denetlenmiştir. PID ve SMC denetleyiciler farklı belirsizliklerin varlığında test edilmiştir. Helikopter modeli, sabit bir ekseninde dönebilen, bir ucunda fırçasız doğru akım (DC) motorunun sürdüğü bir pervane, diğer ucunda ise yük bulunan bir hareketli koldan oluşmaktadır. Önerilen denetim yöntemleri 1-DOF helikopter modelinin denetim başarımını iyileştirmek için kullanılmıştır. Dönme açısını ölçmek için potansiyometre, bilgisayardan elektronik hız denetimcisine (ESC) sinyal göndermek için ise DAQ-6353 kartı kullanılmıştır. Başarımlar, kol açısının istenen ayar noktasını ne kadar hızlı takip ettiği ve aynı zamanda sabit durum hatası ile bağlantılı olarak incelenmiştir. Sonuçlar SMC ile istenen gürbüzlüğün daha iyi sağlandığını ve denetim başarımının PID ile kıyaslandığında daha iyi olduğunu göstermiştir.

Anahtar kelime: 1-DOF helikopter, PID, SMC, Fırçasız DC motor.



"To my Family"

ACKNOWLEDGEMENTS

I acknowledge with sincere gratitude and appreciation my supervisor Assist. Prof. Dr. Tolgay KARA for his support, guide, excellent advise and cooperation throughout the thesis, step by step to complete this project.

I would like to thank all academics in Electrical and Electronic faculty, they are all supportive and friendly.

My appreciations to my family, for their support and encouragement all the time.

TABLE OF CONTENTS

	Page
ABSTRACT	v
ÖZET	vi
ACKNOWLEDGEMENTS	viii
TABLE OF CONTENTS	ix
LIST OF TABLES	xi
LIST OF FIGURES	xii
LIST OF SYMBOLS / ABBREVIATIONS	xv
CHAPTER ONE	
INTRODUCTION	1
1.1 Overview.....	2
1.2 Mechanics and Control Theory.....	3
1.3 Related Works.....	3
1.4 Aim of the Work.....	4
1.5 Thesis Layout.....	5
CHAPTER TWO	
THEORETICAL CONCEPT OF 1-DOF CONTROL	6
2.1 Helicopter Degree of Freedom (DOF) System Concepts.....	6
2.2 Mathematical Model of Helicopter.....	6
2.3 1-DOF Model of Helicopter.....	8
2.4 1-DOF Control Methods.....	10
2.4.1 PID Controller.....	10
2.4.2 Linear Quadratic Tracker.....	12
2.4.3. Sliding Mode Controller (SMC).....	14
2.5 Performance Measures.....	18
CHAPTER THREE	
THE PROPOSED SYSTEM DESIGNS	21
3.1 Introduction.....	21
3.2 The proposed System Structure.....	21
3.3 Hardware Components.....	22

3.4 Software Design.....	25
3.4.1 System Modeling.....	26
3.4.2 Control System Design.....	26
3.4.2.1 PID Controller.....	27
3.4.2.2 Modelling Controller in LabVIEW.....	28
3.4.3 Modelling Block Diagram.....	29
3.4.3.1 PID Block Diagram.....	29
3.4.3.2 SMC Block Diagram.....	30
3.4.3.3 Graphical User Interface (GUI).....	30
CHAPTER FOUR	
RESULTS AND DISCUSSION.....	32
4.1 Operation Results	32
4.2 System Balance Results.....	34
4.3 PID Controller.....	34
4.4 Sliding Mode controller.....	39
CHAPTER FIVE	
CONCLUSIONS AND FUTURE WORKS.....	45
5.1 Conclusions.....	45
5.2 Future works.....	45
REFERENCES.....	46

LIST OF TABLES

Page

Table 3.1 Hardware components: parameters.....25

Table 4.1 Mean square error comparison of PID and SMC controllers.....42



LIST OF FIGURES

	Page
Figure 2.1 Description of the DOF of the helicopter, along with the moments and forces, because of the tail and main rotor and the gravity.....	7
Figure 2.2 Pitching axis a structure	9
Figure 2.3 Block diagram for a feedback system with Classical PID controller....	10
Figure 2.4 Timing diagram for optimal control explain $P(t)$ that original solved By Riccati differential equation.....	13
Figure 2.5 LQT control architecture.....	13
Figure 2.6 SMC Phases	13
Figure 2.7 Phase Trajectory	16
Figure 2.8 Peak Time Overshoot, Settling Time, And Steady-State Error.....	19
Figure 3.1 Proposed 1-DOF helicopter structure.....	20
Figure 3.2 UAV Brushless Motor A2212/10 1400KV.....	22
Figure 3.3 XXD HW30A ESC.....	23
Figure 3.4 Rotary Potentiometer Circuit Diagram.....	23
Figure 3.5 NI-6353 DAQ.....	24
Figure 3.6 Closed-Loop System block diagrams with PD controller.....	28
Figure 3.7 LabVIEW block diagram for modeling the 1-DOF helicopter.....	28
Figure 3.8 PID controller for 1-DOF helicopter in LabView.(LabView block diagram).....	28
Figure 3.9 LabView block diagram for the SMC controller for 1-DOF helicopter.	29
Figure 3.10 LabView GUI for SMC controller for 1-DOF helicopter.....	29

Figure 4.1 The mode selection and real-time monitoring from GUI for proposed 1-DOF helicopter.....	32
Figure 4.2 1-DOF helicopter balance through operation	33
Figure 4.3 Tracking signal by using PID process variables of 1-DOF helicoptered when balancing mass moves to slider's at the end of motor side.....	33
Figure 4.4 Control Input $u(t)$ by using PID process variables of 1-DOF helicoptered when balancing mass moves to slider's at the end of motor side.....	34
Figure 4.5 Error Signal by using PID process variables of 1-DOF helicoptered when balancing mass moves to slider's at the end of motor side.....	34
Figure 4.6 Tracking Signal by using PID Process Variable of 1-DOF helicoptered when balancing mass moves to slider's end that is near balancing block.....	35
Figure 4.7 Control Input $u(t)$ by using PID Process Variable of 1-DOF helicoptered when balancing mass moves to slider's end that is near balancing block.....	35
Figure 4.8 Error signal by using PID Process Variable of 1-DOF helicoptered when balancing mass moves to slider's end that is near balancing block.....	36
Figure 4.9 Tracking Signal by using PID Process Variable of 1-DOF helicoptered when balancing mass changed at the center.....	36
Figure 4.10 Control Input $u(t)$ by using PID Process Variable of 1-DOF helicoptered when balancing mass changed at the center.....	37
Figure 4.11 Error signal by using PID Process Variable of 1-DOF helicoptered when balancing mass changed at the center.....	37
Figure 4.12 Tracking Signal by using SMC Process Variable of 1-DOF helicoptered when balancing mass centered at slider's at the side of motor.....	38
Figure 4.13 Control Input $u(t)$ by using SMC Process Variable of 1-DOF helicoptered when balancing mass centered at slider's at the side of motor.....	38

Figure 4.14 Error signal by using SMC Process Variable of 1-DOF helicoptered when balancing mass centered at slider's at the side of motor.....	39
Figure 4.15 Tracking Signal by using SMC Process Variable of 1-DOF helicoptered when balancing mass moves to slider's end that is Near balancing block.....	39
Figure 4.16 Control Input by using SMC Process Variable of 1-DOF helicoptered when balancing mass moves to slider's end that is near Balancing block.....	40
Figure 4.17 Error Signal by using SMC Process Variable of 1-DOF helicoptered when balancing mass moves to slider's end that is near balancing block.....	40
Figure 4.18 Tracking Signal by using SMC Process Variable of 1-DOF helicoptered when mass changed that located at the center of Motor side.....	41
Figure 4.19 Control Input $u(t)$ by using SMC Process Variable of 1-DOF helicoptered when mass changed that located at the center of motor side	41
Figure 4.20 Error Signal SMC Process Variable of 1-DOF helicoptered when mass changed that located at the center of motor side	42

LIST OF SYMBOLS / ABBREVIATIONS

1-DOF	One Degree Of Freedom
DAQ	Data Acquisition
E(t)	Error Signal
ESC	Electronic Speed Controller
ESS	Steady State Error
F_h	Lifting force of Brushless DC motor
GUI	Graphical User interface.
J_e	Pitching axis rotational inertia
KD	Constant gain of Derivative part of PID controller
KI	Constant gain of an Integral part of PID controller
KP	Constant gain of proportional part of PID controller
L1	Distance from pivot to equilibrium mass
L2	Distance from pivot to Brushless DC motor
M_h	Mass of brushless DC motor
PID	Proportional Integral Derivative
PO	Percentage overshoot.
R(t)	Desired Input
S	Switching surface function.
SMC	Sliding Mode Controller
T_p	Peaking Time
U(t)	Control Input
UAV	Unmanned Aerial Vehicle, commonly known as a drone
W_n	Natural frequency
Y(t)	Output Signal (output angle)
(ξ)	Damping Ratio

CHAPTER ONE

INTRODUCTION

1.1 Overview

The flight principals and the development of helicopters and aircraft have all the time taken a great interest for people. With the improvement of modern computers technological and the advancement in modern control principles and development of automatic control systems, this brings a significant factor for the development of a wide range of new flying vehicles [1-3].

Helicopters when compared with the fixed-wing aircraft, have a specific advantage in regards to maneuverability: Helicopters can fly for long periods of time, identify vertical flight trajectories such as Directory Vertical Take-Off and Landing (VTOL), they are capable of flying sideways, backward, and carry out extreme agile moves at both low and high airspeed. These features allow helicopters to achieve a wide range of tasks that cannot be performed with other aircraft. There is a wide range of functions that can be performed with helicopters such as firefighting, military missions, construction and transportation, search/rescue operations, which are often achieved in urban environments. Even so, helicopters are relatively complex and nonlinear systems, naturally unstable. This is usually because of a highly coupled rotor-body discussion, which gives a boost to a range of inter-axis couplings of their response. This performance makes helicopter piloting a very challenging job, with an excellent workload for the pilot, specifically in cases of low light, high crosswinds or rapid combat. For this cause, the implementing of stability augmentation systems (SASs) that can change from mechanical stabilization units to Automatic Flight Control Systems (AFCSs) is essential to ensure effectiveness and safety in helicopter operation. The capacities pointed out above clearly explain the expenses required to develop a control strategy for these kinds of highly complex systems [7,18,25,29].

Like any technology, the helicopters also have some drawbacks when compared with fixed-wing aircraft. There are less safe, noisier, highly vibrating systems and

significantly harder to fly. Definitely, due to these aspects, the aeronautical society is greatly more focused on fixed-wing research than the alternative rotary-wing. Keeping in mind the significant role of helicopters nowadays and the continual need for advanced study and development in the dynamics and control area of rotorcraft. This work is focusing on the design of an automatic control system for the regulation and tracking of the desired angle with respect to horizontal that a simple single-degree-of-freedom (1-DOF) helicopter model with one propeller exhibits as it freely rotates around a pivot point.

This modelling and control tools used can be applied to many similar control areas in aerospace with position control of helicopters and airplanes to marine industries such as dynamic position control for ships.

1.2 Mechanics and Control Theory

Mechanical systems control is presently among one of the most effective fields of research because of the varied applications of mechanical systems in human life. Even though the study of mechanical systems is going back to Euler and Lagrange in the 1700 decade, it had not been till 1850 decade, in which the mechanical control systems showed up at the picture in regulations of steam engines. In the past century, a series of military, industrial, and scientific applications encouraged control design with rigorous analysis of mechanical systems.

Theoretically complex nature of behavior analysis of nonlinear dynamical systems let many mathematicians research in control systems. Therefore, the efforts of scientists and engineers together resulted in designing Adaptive Control, Linear Control, Nonlinear Control, and Optimal Control theories. Lately, the theory of Robust Control has been placed to the above picture due to a significant need to deal with the existence of uncertainties in real-life control systems. Before the creation of many of these theories, humans handled to satisfy their dream to fly and traveling in the space. It is one of the very best achievements of control engineers and scientists in the first half of the past century. Robotics Systems along with Aerospace Vehicles that required the ability to check out the surface of other planets continue to be among the most complicated machines developed by humans. Over the past of 50 years, Robotics and Aerospace applications continued to be as some of the most important sources of determination for control and rigorous analysis of both

nonlinear and mechanical systems. The improvements achieved by researchers in mechanics and nonlinear control theory mutually enhanced and affected one another [21].

1.3 Related Works

Dolinsky and Jadlovská conducted experimental identification and control of laboratory helicopter model. They identify the system with back-box model, discrete input/output auto-regressive moving average model with external input (ARMAX) and its state space equivalent is used. They use control algorithm design based on the input/output model [13].

Hoc explores two different strategies in the helicopter system identification. The mathematical model of the helicopter is utilized for the control functionality of Linear Quadratic Gaussian (LQG), Model Predictive Control (MPC), Proportional Derivative Control (PD), and Proportional Integral Derivative Control (PID). The controller's performances are compared mutually throughout the step responses with the common amplitudes. The interconnection in real time of the virtual reality model of a helicopter with the real helicopter system improves the flight impression. The control design robustness is checked out by the response of the system throughout the flight to the outside disturbances. Through the control activity, they summarize and review all the obtained results. This study shows the identification of all three working points to be appropriate [14].

Dumanay et al. designed the PID and SMC controller by used LabVIEW and tools. The DC motor is rotated at the preferred speed by controlling the H-bridge by using the Data Acquisition card (DAQ). The experimental setup utilizes DC motor, H-bridge, N-6024E DAQ card, encoder, and LabVIEW software. A variable Pulse Width Modulation (PWM) signal has been used at the PID control, and a constant ($\pm 5V$) amplitude voltage is supplied the DC motor. The controllers' performances have been examined when the disturbance effect has applied to the motor shaft by using a relay for two seconds. Later, the experimental results have been compared to one another. The SMC and PID controllers reach their particular reference speeds at around 1 second and 15 ms when the disturbance effect has applied to the motor. Even though SMC gets to its reference speed very faster, it has a chattering problem

with the motor. This drawback can be removed by using some strategies that eliminate the chattering [7].

Nilsen designed and constructed multiple two degree of freedom (2-DOF) helicopter models. He developed a mathematical model for controller and simulation development MPC and PID controllers have been designed based upon the mathematical model. The mathematical model has been developed by using the parameters discovered by conducting experiments on the real system and they were used successfully to develop the PID controllers for the proposed system. The experiment results show that the developed PID controller was able to control the model of the real helicopter to setpoint over a reasonable time and held the pitch angle at set point with frequent movement about 3 degree offset point due to random disturbances. The 2 DOF model is linearized and a Kalman filter has been configured for the MPC controller, however, because of unexpected problems with Simulink and absence of time, no MPC controller has been developed [28].

1.4 Aim of the Work

The primary purpose of this thesis is to design and implement an automatic control system for the regulation and tracking of the desired angle with respect to horizontal that a simple 1-DOF helicopter model with one propeller exhibits as it freely rotates around a pivot point.

A 1-DOF mechanical laboratory-size helicopter model can just be constructed using a rod that can rotate freely around a pivot point with a propeller connected on one end. The idea is to control the angle of the rod with respect to horizontal using the lifting force generated by the propeller, which can represent a simplified model of the motion of a helicopter where the altitude is assumed to be fixed and attitude is controlled for one axis only. The idea is to be able to represent the angle of a helicopter to earth during flight by this variation of the angle of the rod with respect to horizontal. The mechanism is constructed that allows angle movement around pivot point with the presence of one motor to regulate or track specific desired angle despite disturbances and load variations. Brushless DC motor with propellers is used to give positive elevation force on the propellers side. In this study, two most suitable control strategies of PID and SMC are tested to find the best-suited controller and to verify the experimental and simulated results [4,20].

1.5 Thesis Layout

This thesis is organized in four chapters besides this chapter and ends with references, where Chapter two explains the Degree Of Freedom (DOF) concepts of the helicopter and the control strategy. Chapter three describes the design of a 1-DOF helicopter with all techniques and steps used in it. In Chapter four the experimental results are presented and discussed. Finally Chapter five summarizes the main points achieved in this thesis, and suggests some improvements that can be studied in the future work.



CHAPTER TWO

THEORETICAL CONCEPT OF 1-DOF CONTROL

2.1 Helicopter Degree of Freedom (DOF) System Concepts

The helicopter is a very complex system and it is hard to build a flight dynamics model for it with high efficacy since the helicopter aerodynamic phenomenon is very complicated. There is an aerodynamic interference between horizontal tail, vertical tail, main rotor, tail rotor, and fuselage. Furthermore, each DOF of the helicopter is hugely coupled. Regular theoretical modeling approaches build a flight dynamics model of helicopter depending on several physical laws. However, to be able to apply these physical laws to helicopter model the helicopter model always requires making a lot of assumptions. As a result, the accuracy of the flight dynamics model for helicopter constructed by theoretical methods is even now not good enough yet. Even though it is necessary to continue enhancing conventional techniques, various other modeling methods based on modern techniques including system identification are usually needing to be developed [5,11].

2.2 Mathematical Model of Helicopter

We have considered that the helicopter is a rigid body. A coordinate system of the body is centered in origin at the helicopter center of gravity. The helicopter coordinate system and the balance parameters consist of various factors that are effective on movement and stability of the helicopter. These parameters involve the angle of rotation, distance, masses, and inertia. These parameters and coordinates are dependent on the DOF used in the model. There are several types of DOF helicopter such as 1-DOF Helicopter, 2-DOF Helicopter, 3-DOF Helicopter, 6-DOF Helicopter, and such. Figure 2.1 shows the DOF of the helicopter [6].

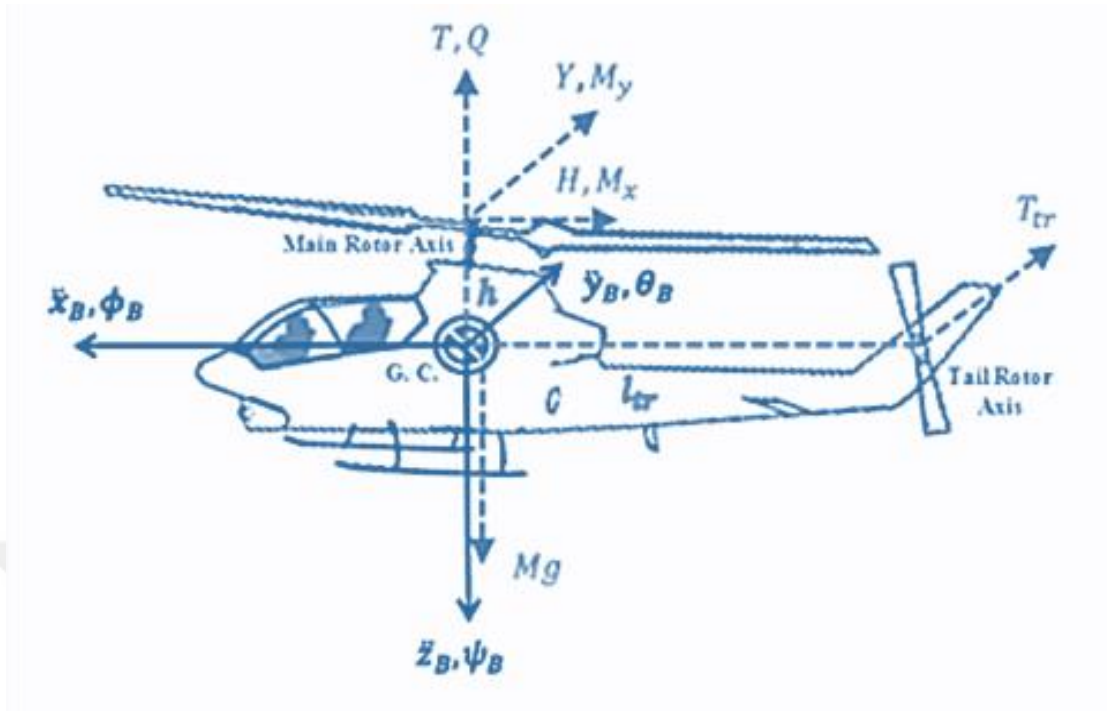


Figure 2.1 Description of the DOF of the helicopter, along with the moments and forces, because of the tail and main rotor and the gravity. [6]

In the following the specification of DOF helicopter system parameters is presented.

Coordinate System of Helicopter:

- x_B : The x axis, which is 0 at the center of gravity.
- y_B : The y axis, which is 0 at the center of gravity.
- z_B : The z axis, which is 0 at the center of gravity.

The distances in helicopter coordinate system (shown in Figure 2.1) includes:

- h : The distance from the main rotor head to the center of gravity.
- l_{tr} : Distance between center gravity of helicopter and the tail rotor.

Rotation Angles of helicopter consist of three values each on rotate on one axis, so the system rotates together with the rig over the elevation and travel axes. The platform is fixed in the mount at the center of gravity. For helicopter position there are three angles are used (shown in Figure 2.1), which are:

- **Pitch Angle (θ_B)**: The rotational angle in which the helicopter is rotated over the lateral axis. It is zero when the helicopter is horizontal.
- **Euler's angles - Roll (ϕ_B)**: The rotational angle in which the helicopter is rotated over the longitudinal axis. It is zero when the arm is horizontal.

- **Yaw Angle (ψ_B):** The rotational angle in which the helicopter is rotated over the vertical axis.

The Rotational Inertias are defined as:

- Roll Axis Inertias (I_x)
- Pitch Axis Inertias (I_y)
- Yaw Axis Inertia (I_z)

Masses and momentum of helicopter also has forces and moments which acting upon the helicopter. The effects of the moments and forces that initiated by the fuselage, the vertical and horizontal stabilizer are neglected. These forces and momentum (shown in Figure 2.1) includes [26]:

- Lateral force (Y)
- Longitudinal force (H)
- The Gravity Force (M_g)
- The Main Rotor Traction Force (T)
- The Tail Rotor Traction force (T_{tr})
- The Roll Moment (M_x)
- The Roll Moment (M_y)
- The Pitch Moment (Q)
- The Motor Pair Moment or Yaw Moment (Q)

2.3 1-DOF Model of Helicopter.

One-degree of freedom helicopter is an articulated arm along with a motor placed at one end, which is connected to a propeller that provides less or more lift in function of the power supplied of the motor. Potentiometer at the joint's axis returns a voltage according to the angle. Therefore, the control variable will be the lift propeller (voltage given to the motor), and the output variable will be the axis position (voltage sent by the potentiometer). As a result, the physical interface, an input variable, and a control loop are needed. Figure 2.2 shows the 1-DOF helicopter structure. As this thesis is focused on a study the controlling balance for 1-DOF helicopter, thus the main rotational axis that needs to study is pitch axis balancing control [19, 26]. The pitching axis a structure is illustrated in Figure 2.2.

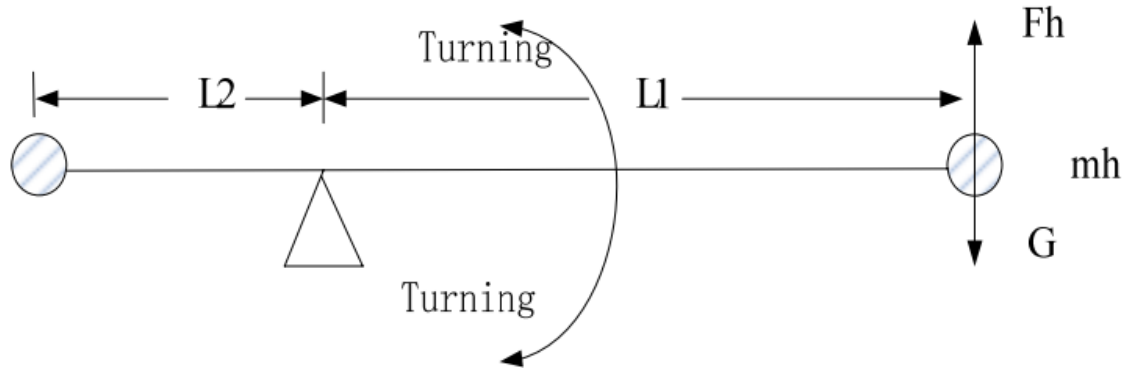


Figure 2.2 Pitching axis structure

One propeller motor making the direct lift generates the pitching axis torque. The helicopter rises in case that the direct lift is higher than gravity and otherwise it drops. By assuming that the helicopter is hung-up in the air and the degree of the pitch is zero; the equations can be given as follows [30,32,33].

$$J_e \ddot{\theta} = F_h l_1 - l_1 G \quad (2.1)$$

Where J_e , is the pitching axis rotational inertia; $\ddot{\theta}$ is the pitching axis rotation acceleration; F_h is a direct lift of motor; l_1 is the distance from motors to fulcrum; G is the gravity.

The direct lift of the motor can be calculated from the following equation:

$$F_h = K_c V_m \quad (2.2)$$

Where K_c is the blades motor lifting constant; V_m is the motor voltage. The effective gravity torque T_G causes by pitching axis gravity is

$$T_G = l_1 G \quad (2.3)$$

Thus, by subtracting equations (2.2) and (2.3) in 2.1 we get

$$J_e \ddot{\theta} = K_c V_m l_1 - T_G \quad (2.4)$$

In cases where gravity disturbance torque is neglected, the transfer function of this system part can be computed by the following equation:

$$\frac{\varepsilon(s)}{V_m} = \frac{K_c l_1}{J_e s^2} \quad (2.5)$$

The equation (2.5) can be specified in term of current to be

$$\frac{\theta(s)}{I_s(s)} = \frac{K_c l_1}{J_e s^2 + K_f s} \quad (2.6)$$

2.4 1-DOF Control Methods

Many control methods can be used in control strategy of 1-DOF systems, such as PID, (LQR), and SMC.

2.4.1 PID Controller

The easiest way of implementing a controller is by using a PID controller. It does not need to the higher knowledge of the system and it can balance the majority of a system that is controllable. There are three principal methods of looking at the PID controller. The first method is the classical control method. The PID controller gives two poles and two zeroes to a system that can be utilized to insert new dominant poles into the system or cancel existing poles from it. The second method is related to the first method, it weights the several frequency components of the error depending on the location of poles and zeroes of the PID controller. The last way is that it makes a new input depending on the change of the error rate, the error's weighted sum, and the error integral [7].

Fig. 2.2 shows the analog PID control system structure that used with the analog control system. This system is composed of a controlled plant and the analog PID controller.

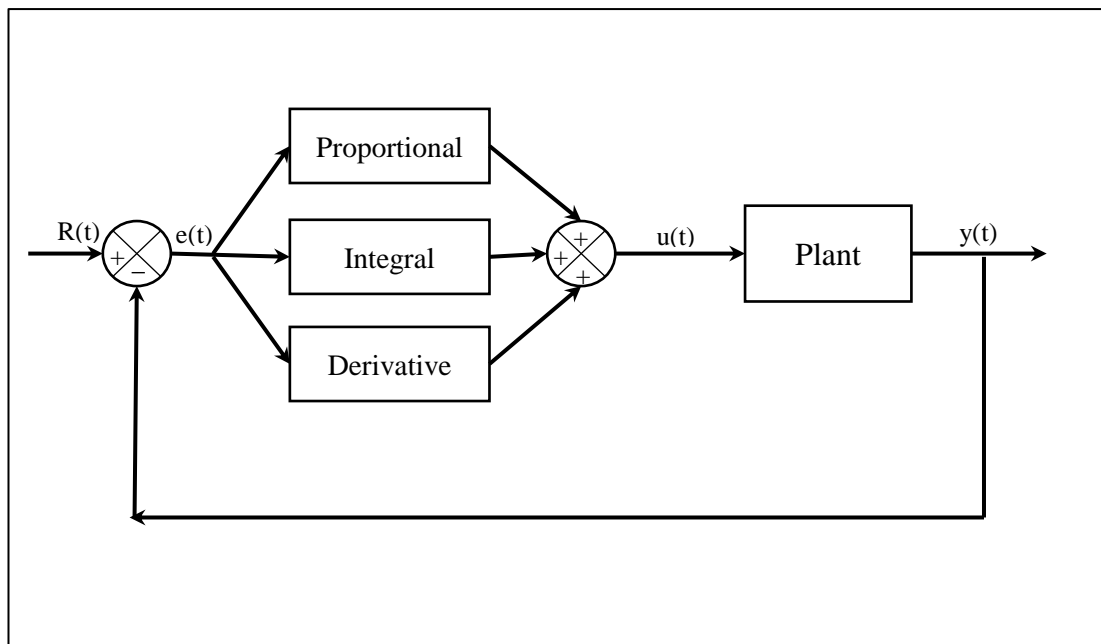


Figure 2.3 Block diagram for a feedback system with Classical PID controller

The PID controller is the type of linear controller; the error is calculated by the given value of $r(t)$ and the actual output $y(t)$.

$$e(t) = r(t) - y(t) \quad (2.7)$$

The value of PID control is gained by linearly composing the integral proportion and error differential that control the controlled plant, therefore it is referred to us as PID controller. The law of proportional control is as follows:

$$u(t) = k_p e(t) = k_p (r(t) - y(t)) \quad (2.8)$$

Where k_p is the gain. It basically raises the control variable once the control error is larger. Nevertheless, it presents the steady state error of the system. The integral action can be calculating in the following equation.

$$u(t) = k_i \int_0^t e(\tau) d\tau \quad (2.9)$$

Where k_i is the integral gain.

As the proportional action handles the error of current value, and the integral action handles the past values, also, the derivative action is based upon the forecasts of the error future values. The derivative action expression is:

$$u(t) = k_d \frac{de(t)}{dt} \quad (2.10)$$

Where k_d is the derivative gain. We can present the combination of integral actions, derivative and proportional via the following transfer function:

$$C_i(s) = k_p \left(1 + \frac{1}{T_i(s)} + T_d s \right) \quad (2.11)$$

Where T_i is the integral action time constant and T_d is the derivative action time constant [7].

2.4.2 Linear Quadratic Tracker

The design procedures of Linear Quadratic Tracker (LQT) have a philosophy and usage that are much the same as the methodology of LQR. The theory is to find a controller that gives the best possible efficiency concerning several given measure of effectiveness. Selecting the gains using a strategy that is considered to be perfect in linear case is also beneficial and preferable to choosing the gains utilizing the trial and error as in PID control. The property of robustness is what is required for the

landing problem, as the challenge involves wind disturbance. Not very much improvement in the cases was not to have wind disturbance; even so, under wind disturbance, the performance of LQT controller is thought to be better than PID in settling and response time. A quadratic function defines the case in which a linear differential equation set defines the system dynamics and the cost is known as the LQR problem. The LQR problem can be stated for a system of continuous linear time-invariant is defined by [31]:

$$\dot{x}(t) = Ax(t) + Bu(t), \quad (x(t=0) = x_0, \quad x(t) \in R^n, u(t) \in R^m) \quad (2.12)$$

$$j = \frac{1}{2} \int_0^{\infty} [x^T Qx + u^T Ru] dt \quad (2.13)$$

Then a control law can be described to reduce the cost functional. If specific conditions are satisfied, LQR guarantees nominally steady closed loop systems and accomplishes guaranteed levels of stability robustness.

The LQR controller is developed specially to drive the states to 0; even so, the controllers are required to track a reference input. This qualification comes from the architecture of the landing system. In the architecture of the landing system, the block of the high-level system produces the necessary roll angles, total airspeed and reference altitude for the aircraft to continue track. Even so, the aircraft requires the angles concerning the control surfaces to modify attitude. The controller block performs this conversion, however, the reference commands must be tracked effectively to be able to follow the preferred landing trajectory. For this goal, the cost function is customized in a way that it contains the monitoring error, not the states. The optimal control and cost function are obtained in follows:

$$j = \frac{1}{2} \left(y(t_f) - r(t_f) \right)^T P \left(y(t_f) - r(t_f) \right) + \frac{1}{2} \int_0^{t_f} \left[\left(y(t) - r(t) \right)^T Q \left(y(t) - r(t) \right) + u^T Ru \right] dt \quad (2.14)$$

Where $r(t)$ is the reference command, $y(t)$ is the output of the system, t_f is the final time.

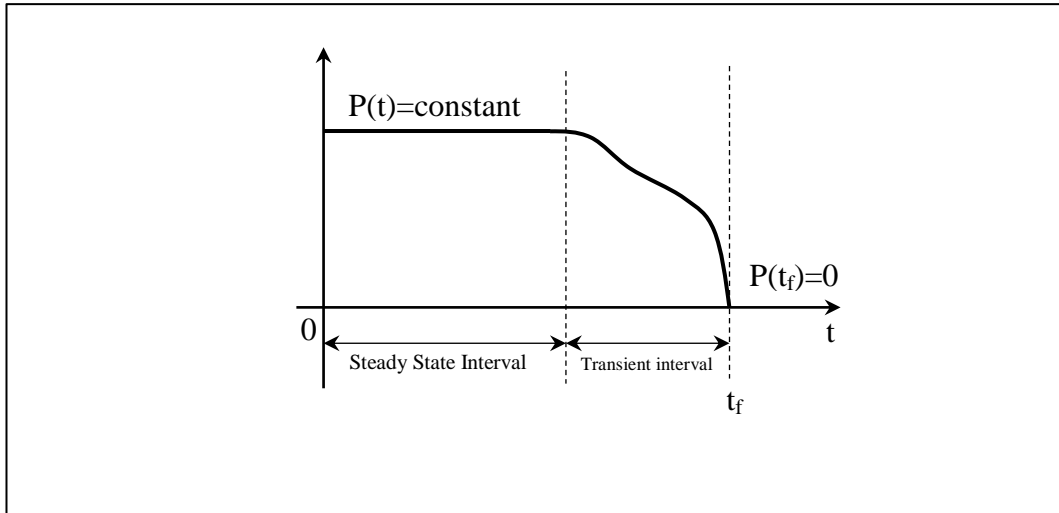


Figure 2.4 Timing diagram for optimal control explain $P(t)$ that original solved by Riccati differential equation

In a real system, the states can be measured by using sensors that expose delay to the system. Furthermore, often some states are not able to measure if the appropriate sensors are not installed to the system or the installed sensors fail to give the necessary parameters. All those missing parameters are acquired through calculation (observer) by using other states, which means extra delay. The LQT control block diagram is shown in Figure 2.5.

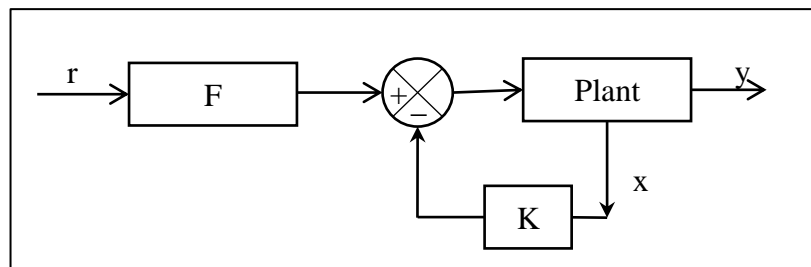


Figure 2.5 LQT control architecture

2.4.3 Sliding Mode Controller (SMC)

In control principles, the SMC is a type of variable structure control (VSC). SMC is a non-linear control method that changes the dynamics of a non-linear system by the approach of hi-frequency switching control. The law of VSC gives a robust and effective means of nonlinear controlling nature. It is invariant to corresponding disturbances and uncertainty. The SMC variable structure allows it to adapt to

parameter disturbances “instantly.” In systems of variable structure, the control is permitting to modify its structure, to switch at any time from one to another.

The problem in the design of the variable structure is how to choose the parameters of each one of the structures and to determine the switching logic. Thus, the multiple control architectures have been designed so that trajectories constantly move toward a switching state, therefore the ultimate trajectory is not going to exist totally within one control structure. Rather, the ultimate trajectory is going to slide along the control structures boundaries. The system motion that slides along these boundaries is known as a sliding mode and the geometrical situation consisting of the boundaries is known as the sliding surface. Figure 2.6 shows the SMC phases [12,15,16].

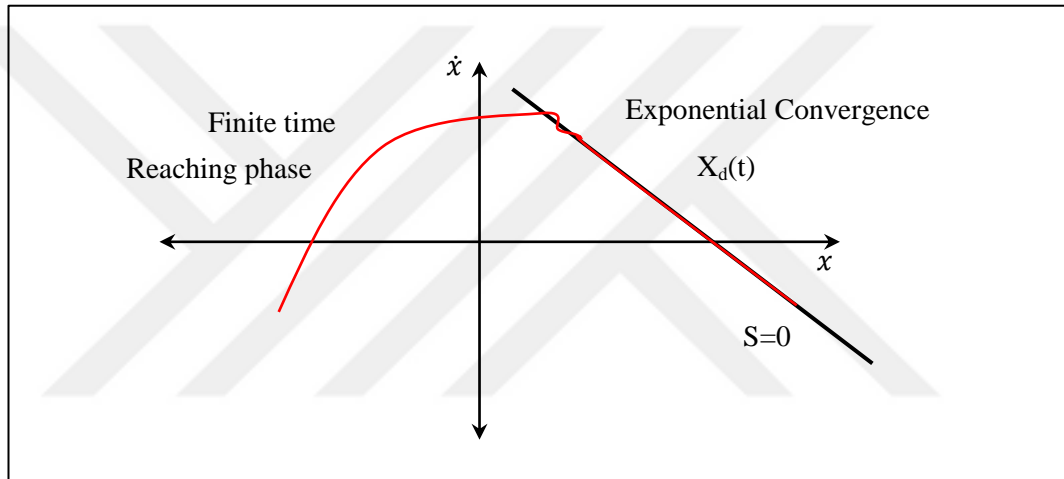


Figure 2.6 SMC phases

Figure 2.6 represents the behavior of controlled systems. By proper design of the sliding surface, VSC achieves the regular goals of control, for example, regulation, stabilization, disturbance rejection, tracking, and such.

2.4.3.1 Sliding Surface Design

SMC is based on the idea of variable structure control. The following equation gives the plant equation:

$$\ddot{\theta}(t) = -f(\theta, t) + b \times u(t) \quad (2.15)$$

The first point is to define “sliding surface”, which is a set of dynamics described by the designed in which the controller will make the system to act. The typical form for the sliding surface is given by equation (2.16):

$$s = c \times e(t) + \dot{e}(t) \quad (2.16)$$

Where s is the sliding mode, where c must satisfy Hurwitz condition $c > 0$, then \dot{s} will be :

$$\begin{aligned}\dot{s}(t) &= c \times \dot{e}(t) + \ddot{e}(t) = c \left(\dot{r} - \dot{\theta}(t) \right) + \left(\ddot{r} - \ddot{\theta}(t) \right) \\ \dot{s}(t) &= c \left(\dot{r} - \dot{\theta}(t) \right) + \left(\ddot{r} + f(\theta, t) - b * u(t) \right)\end{aligned}\quad (2.17)$$

Sliding mode based on reaching law consists of two-part reaching phase and sliding phase. The reaching phase controller has the aim to maintain the system stability manifold and the sliding phase controller target the system to be sure it be on a slide to equilibrium. The sliding mode controller based on reaching law can be illustrated in Figure 2.7.

There are three types of reaching law as follow:

- 1- Constant rate reaching law

$$\dot{s} = \varepsilon \times \text{sgn}(s), \text{ where } \varepsilon > \text{zero} \quad (2.18)$$

ε is a positive constant, its effect on the performance of the system. Choosing a small value of ε will make the system take too long reaching time, on the other hand, a large value of ε will cause chattering in the system response.

- 2- Exponential reaching law

$$\dot{s} = -\varepsilon \times \text{sgn}(s) - k \times s \quad (2.19)$$

Where $\varepsilon, k > \text{zero}$, the proportion part $k \times s$ force the system to be faster to arrive switching surface when the value of s is too high.

- 3- Power rate reaching law

$$\dot{s} = -k \times |s|^\sigma \times \text{sgn}(s) \quad (2.20)$$

This law for reaching phase will make the response faster when the error is too large, in another word when the state is far from the switching surface it will cause a faster reaction and low chattering.

- 4- General reaching law.

$$\dot{s} = -\varepsilon \times \text{sgn}(s) - f(s), \quad \varepsilon > \text{zero} \quad (2.21)$$

All the four kinds are following are satisfy the condition $\dot{s} < 0$. Now it is chosen as an exponential reaching law for the design. Substitute equation (2.19) into (2.17),

$$\varepsilon \times \text{sgn}(s) - K \times s = c \left(\dot{r} - \dot{\theta}(t) \right) + \left(\ddot{r} + f(\theta, t) - b \times u(t) \right) \quad (2.22)$$

$$u(t) = \frac{1}{b} \left(c \left(\dot{r} - \dot{\theta}(t) \right) + \dot{r} + f(\theta, t) - (\varepsilon \times \text{sgn}(s) - K \times s) \right) \quad (2.23)$$

A sliding mode controller has two phases, the first is known as the reaching phase. In this phase, the controller is driving the system state upon the sliding surface. The second phase is known as the sliding phase, through which the system state ‘slides’ on the sliding surface. Figure 2.7 shows the phase plane of a 1st order sliding surface.

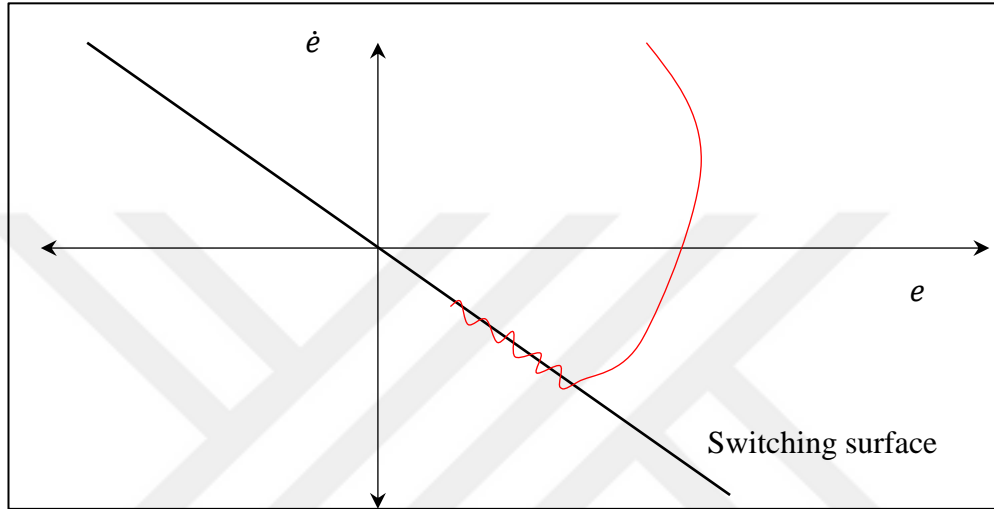


Figure 2.7 Phase trajectory

The sliding surface derivative is equated to reaching law that enforces the robustness of the controller. From Figure 2.7 it can be noticed that if the plant state overshoots the sliding surface it should be forced back onto it. A suitable discontinuity is utilized by the sign function and it is multiplied by a very small positive constant η . Furthermore, to show that Equation (2.21) stabilized the system, and to evaluate the switching gain minimum value, the theory of Lyapunov stability has been used. A Lyapunov candidate is described for a scalar system as in the following equation: (2.24).

$$V = -\frac{1}{2}S^2 \quad (2.24)$$

Taking the derivative of Equation (2.22) to time we get:

$$\dot{V} = -S\dot{S} \quad (2.25)$$

Substituting Equation (2.18) into Equation (2.23) we get:

$$\dot{V} = S \times c \left(\dot{r} - \dot{\theta}(t) \right) + \left[\ddot{r} + f(\theta, t) - b * \frac{1}{b} \left(c \left(\dot{r} - \dot{\theta}(t) \right) + \ddot{r} + f(\theta, t) - (\varepsilon \times \text{sgn}(s) - K \times s) \right) \right] \quad (2.26)$$

If the system parameters are equal to the average values, then equation (2.24) reduced to be:

$$\dot{V} = -S \times \eta \times \text{sign}(S) = -\eta|S| \leq 0 \quad (2.27)$$

A typical sliding mode is available only whenever the state trajectory $x(t)$ regards the controlled plant meets $Sx(t) = 0$ at every $t \geq t_0 = 0$ for some t_0 , which needs infinitely fast switching. In real systems, all facilities sensible for the switching control function have problems such as hysteresis, delay, etc. that force switching to take place at a finite frequency. The associated point then oscillates inside a neighborhood of the switching surface. This oscillation is referred to as chattering. If the switching frequency is very high in comparison to the system dynamic response, the finite switching frequencies and imperfections are frequently but not at all times negligible.

In summary, a significant issue with the sliding mode controller lies in the fact that SMC needs infinite bandwidth. The sign function cannot be implemented in the real world since it requires the control hardware responds instantly. Many methods could be used to mitigate this, such as “Chatter Suppression Techniques”.

2.4.3.2 Chattering Suppression Techniques

Chattering is natural in SMC because of the discontinuous term, $\text{sign}()$. Chattering can cause damage to the system. If the sliding surface crosses over 0 the sign would change producing the $\eta \text{sign}(S)$ term to modify rapidly. This will cause the sliding surface to invert direction and cross back over 0 that in turn makes the $\eta \text{sign}(S)$ term to change once again. This is the phenomenon known as chattering and is due to the fact that SMC needs infinite bandwidth. There are some techniques to reduce chattering, one of them using a quasi-sliding mode that make the state lying in a specific region at the Δ neighborhood, Δ sometimes called boundary layer. There are two methods to implement quasi sliding mode:

- 1- Saturation function instead of $\text{sign}(s)$ function :

$$sat(s) = \begin{cases} 1 & s > \Delta \\ k \times s & |s| \leq \Delta \\ -1 & s < -\Delta \end{cases} \quad (2.28)$$

2- Relay function instead of sign(s) function:

$$\theta(s) = \frac{s}{|s| + \rho} \quad (2.29)$$

Where ρ is a small positive number.

2.5 Performance Measures

The performance measures or criteria are explained for 2nd order systems once the step input is applied. Several performance measures are identified considering the systems. Based on natural frequency (ω_n), damping ratio (ξ) and the performance measures are discovered. Additionally, if the natural frequency and damping ratio are known, then the performance measures can be determined [34].

In cases where step input is applied, the system will give a response according to the damping ratio. By making use of percentage overshoot (PO), the damping ratio can be computed by using the following equation.

$$\xi = \frac{-\ln\left(\frac{PO}{100}\right)}{\sqrt{\pi^2 + \left(\ln\left(\frac{PO}{100}\right)\right)^2}} \quad (2.30)$$

In a stable system, the overshoot is the difference between final output values and maximum values. Ratio overshoot is 100 multiplied by the ratio of overshoot to the final output value. As well, when there is a percentage, graph, overshoot could be calculated, however, if the damping ratio is known, then the other percentage formulas of overshoot can be used.

$$PO = 100 \times \frac{MOV - FOV}{FOV} \quad (2.31)$$

When the damping ratio equals to zero, then the natural frequency is the oscillation frequency of the system. The natural frequency is computed by using the peak time or settling time.

Peak time represent the elapsed time that is the time between applying the step input till it reached to its maximum value. As well, the peak time can be computed with the help of the natural frequency and damping ratio.

$$t_p = \frac{\pi}{\omega_n \times \sqrt{1-\xi^2}} \quad (2.32)$$

The steady state error represents the difference between the values of final output and the reference input. In most cases, it is an undesired situation in which the system response would not settle to reference input. It is referred to as steady state error. In a case where the system has a steady state error, it could be removed efficiently with the aid of an integral type of controller. The general transfer function of 2nd order systems is in follows:

$$t_s = \frac{K\omega_n^2}{s^2 + 2\xi\omega_n s + \omega_n^2} \quad (2.33)$$

System results final value is the limits of the transfer function as “s” goes to zero. With consideration to the transfer function, the final value is K for a unit step input. Figure 2.8 shows the settling time, overshoot, peak time and steady-state error.

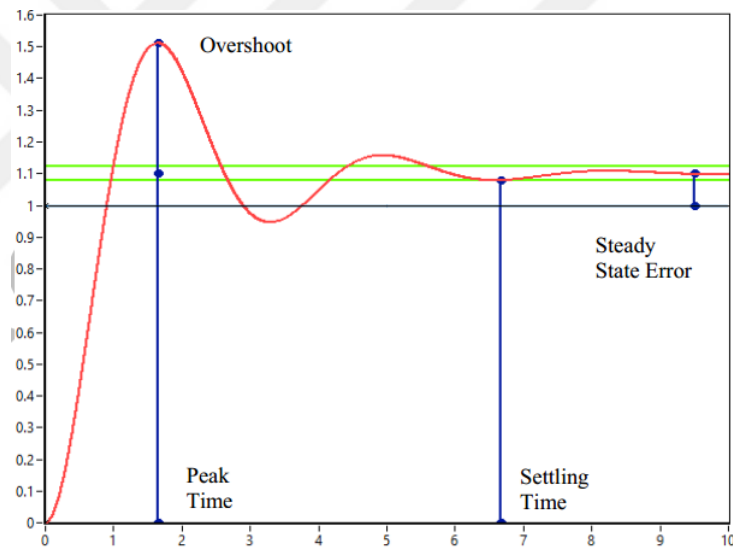


Figure 2.8 Peak time Overshoot, settling time, and steady-state error

CHAPTER THREE

THE PROPOSED SYSTEM DESIGNS

3.1 Introduction

In this study it is aimed to design and control a 1-DOF helicopter model. The speed of DC motor was controlled through the use of PID and SMC. The software was produced through LabVIEW and a (DAQ) card. The feedback signal from the encoder is transferred to the PC via the DAQ card and the controller output sign is given to the ESC again via the same card. While the outputs are obtained as PWM signals in PID control, +5V or -5V is applied to the motor depending on the used signum function in the SMC.

3.2 The Proposed System Structure

The system consisted of mechanical parts, electronic/electric parts, controlling parts and software. The main parts of “1-DOF Helicopter” can be seen in Figure 3.1.

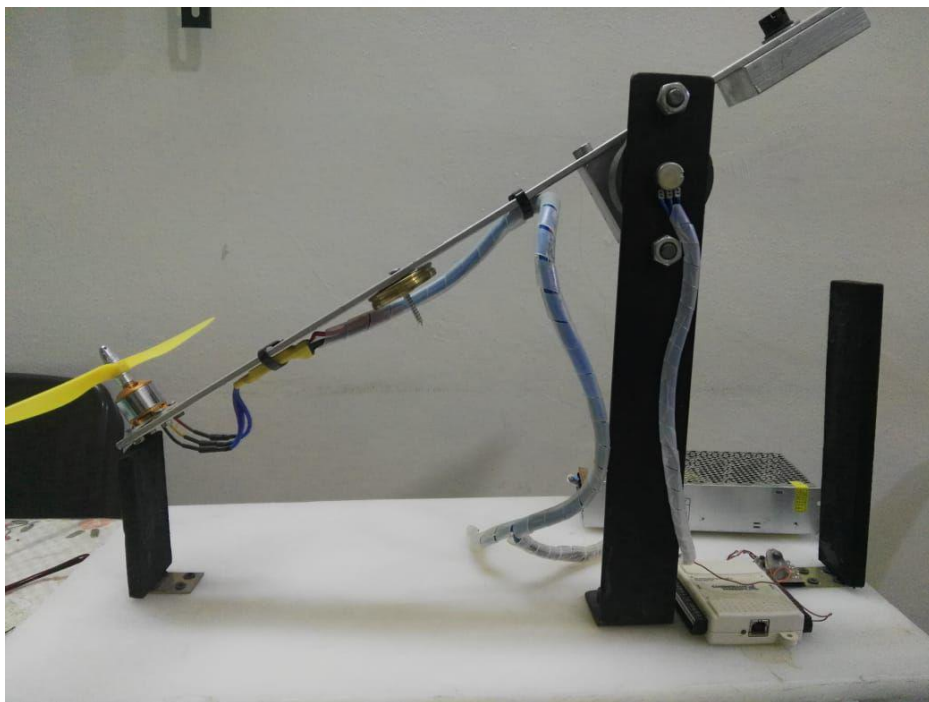


Figure 3.1 Proposed 1-DOF helicopter structure

3.3 Hardware Component:

This part includes the mechanical and electrical component of the proposed system.

3.3.1 Mechanical Parts

The mechanical part includes the metal structure that simulates helicopter structure in term of one free degree of freedom. It consisted from a metal bar of 60cm long. The DC motor and propeller are positioned in one end while the balancing block is positioned in the second end and it can change its position by the slider. This bar is positioned on a metal base and linked with it by movable joint pitching axis in which the joint is a 40cm distance from the end of the motor side and 20cm from balancing block side, and the base is 35cm high. There is also a sliding mass in motor side located in mid-distance between the motor and movable joint which can be slid to change its distance that used to test the system stability. Figure 3.1 shows the mechanical structure and its dimensions.

3.3.2 Electric/Electronic Parts

The electronic and electrical part includes all components that used to simulate the helicopter motion and controls and to gather data, which includes motor, ESC, Potentiometer, DAQ Card, power supply, wiring.

DC Motor

The motor is consisting of a stator and a rotor. The stator is steady whereas the rotor spins according to the applied voltage. In the proposed system we have used brushless DC motor. The main reason for using a brushless DC motor is making the operation more effective, more reliable and less noisy. A brushless dc motor is lighter and has a longer life than a brushed motor that has the same power output and is also much more efficient than a brushed one. A brushless dc motor has a linear torque-speed relationship. For these reasons, a brushless DC motor provides better speed control. The rotor of a motor has a strong permanent magnet and the stator has three coils which are named A, B, and C and have a special arrangement. When the coils are energized, they became electro magnetized. The working principles can be interpreted with the force interaction between the electromagnet and the permanent magnet. If energy is provided to the coil A, the opposite side which are the poles of the stator and rotor attract each other. When the next coil is energized, the poles of

the rotor move to the next one. It is a successive and repetitive process. During this process, the motor continues to run.

The unmanned aerial vehicle (UAV) Brushless Motor model A2212/10 1400Kv has been used which provides excellent performance, quality, and dependability. Manufactured by high-quality components and bearings, this type of brushless motor is one of the most powerful and smoothest in its class. Figure 3.2 shows the UAV Brushless Motor A2212/10 1400Kv.



Figure 3.2 UAV Brushless Motor A2212/10 1400KV

Electronic Speed Controller (ESC)

Electronic Speed Controller is a circuit that is utilized in controlling the power or the speed of an electric motor. An ESC obtains signals from the receiver and modifies the speed and direction of the motor and also serves as a braking system. In this work, we have used XXD HW30A ESC of (5.6V - 16.8V) power input and 30A constant current, and its mass is equal to 25g. Figure 3.3 shows the ESC type XXD HW30A.

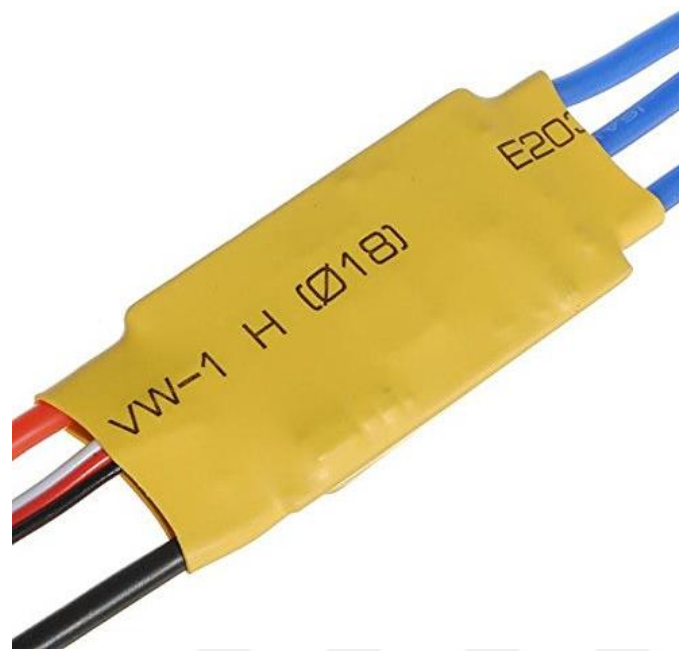


Figure 3.3 XXD HW30A ESC

Rotary Potentiometer

The rotary potentiometer is a rugged, compact, thick-film unit that uses either wire wound elements, or cermet or conductive plastic. It can be used in various applications. It is designed to provide a fairly precision position measurement. As it rotated, the incremental rotary gives just cyclic outputs. Since the rotary potentiometer feature a low cost and the capability to get information about the velocity or position of motion, the most generally utilized of the rotary potentiometer are the gradual rotary encoders.

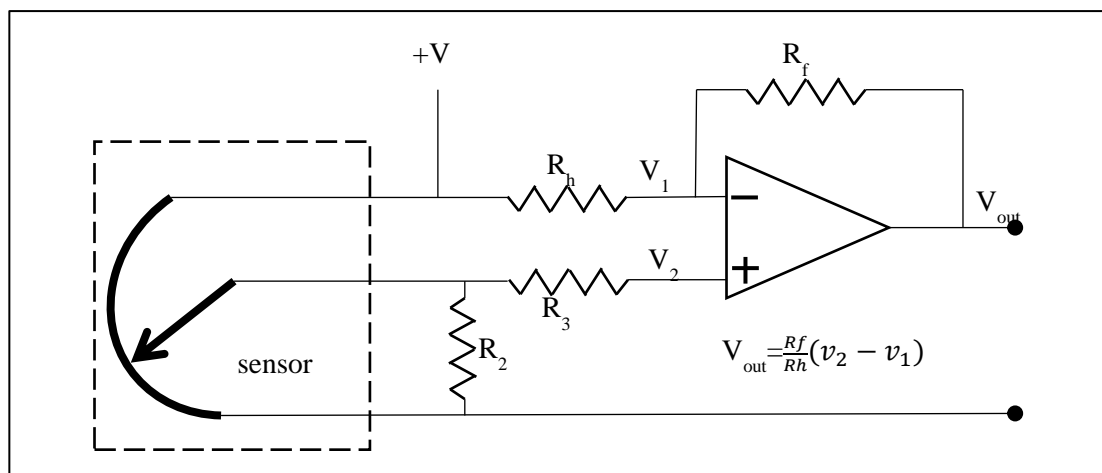
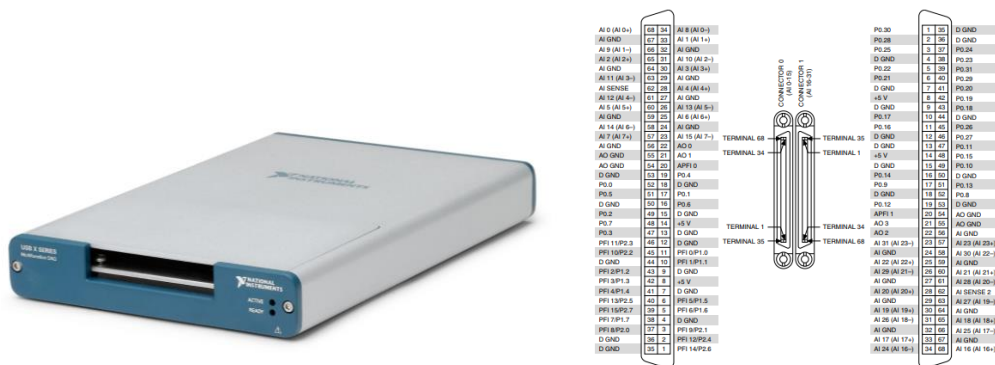


Figure 3.4 Rotary potentiometer circuit diagram

Data Acquisition (DAQ)

Data acquisition or DAQ is the procedure of measuring physical phenomenon or an electrical signal such as sound, pressure, temperature, current or voltage by using a computer. Any DAQ system has DAQ measurement hardware, sensors, and a computer with specific software. In this work, we have used PC-based DAQ systems. There different type of DAQ system includes Pc based DAQ when compared with traditional measurement systems, the PC-based DAQ systems take advantage of the productivity, the high processing power, connectivity, and display. As PC has extremely developed and there is a wide range of PC from low to high-speed processing computer this gives a wide selection of PC with DAQ to providing a flexible, powerful, and affordable measurement solution.

In this work, we have used DAQ from National Instruments (NI) model USB-6353, which are multifunction DAQ modules. It has 32 analog inputs, (16-Bit resolution, 1.25 MS/s), 4 analog output (2.86 MS/s), 48 Digital input/output USB Multifunction I/O Device—The USB-6353 offers analog I/O, digital I/O, and four 32-bit counters/timers for PWM, encoder, frequency, event counting, and more. On-board NI-STC3 timing and synchronization technology deliver advanced timing functionality, including independent analog and digital timing engines. The USB-6353 is well suited for a broad range of applications, from basic data logging to control and test automation. The included Figure 3.5 shows the NI-6353 DAQ.



3.4.1 System Modelling

The physical model of 1-DOF helicopter system described in Chapter 2 section 2.3 has been used to modulate the control balance of the proposed 1-DOF system. The system parameters are taken from real parameters of a hardware component which are explained in Table 4.1. These parameters will be used for obtaining the mathematical model of the 1-DOF Helicopter system. The beam is directly mounted to the encoder to measure the beam angle. When the motor is energized and F_h is greater than the weight of the helicopter $m_h.g$, the helicopter rises [10].

Table 3.1 Hardware component: parameters

Symbol	Definition	Value	Unit
L1	The distance between the balance block and pivot point.	0.0665	m
L2	The distance between the BLDC motor and pivot point	0.303	m
Mh	The total mass of BLDC motor and rotor	0.235	Kg
Mb	The total mass of the balance block	0.66587	Kg
Je	Moment of inertia of the system	0.115	Kg.m ²
g	Acceleration of gravity	9.81	m/s ²
Is	Current of motor	Variable	Ampere

The system transfer function is found as follow:

$$\frac{\theta(s)}{I_s(s)} = \frac{K_c l_1}{J_e s^2 + K_f s} \quad (3.1)$$

$$\frac{\theta(s)}{I_s(s)} = \frac{0.1186}{s^2 + 2.032 s} \quad (3.2)$$

3.4.2 Control System Design

Open loop systems are called the manual control systems as the output does not affect the input. Although open loop structure is simple, economical and stable, it is inaccurate, unreliable and has no disturbance rejection. Closed loop systems are called automatic control systems and they have many advantages like disturbance

rejection, noise attenuation, the presence of nonlinearity and robustness, so the closed loop system are preferred in control applications in general. The purpose of the controller design with a closed loop system is the achievement of the previously specified performance measures. Choosing the type of controller depends on the system objectives and needs. In general, there are three tuning parameters; proportional (P), integral (I) and derivative (D). P-term depends on the present error, I-term accumulates the past errors and D-term predicts the future errors [8,17,23,24].

3.4.2.1 PID Controller

PD controller is generally used for position control applications because of the plant's integrator. It approaches two of closed-loop system poles to desired locations and adds a zero at the same time while it does not change the order of the system. PD controller adds one zero to the system. When the step input is applied at the beginning, the derivative of the initial error approaches infinite in a split second. This pulse is described as a derivative kick. Design of the PD controller on the forward path results in a derivative kick. The other disadvantage of a PD controller is that it cannot reject disturbance and eliminate the steady state error. Closed loop system block diagrams with a PD controller can be seen in Figure 3.6 [9].

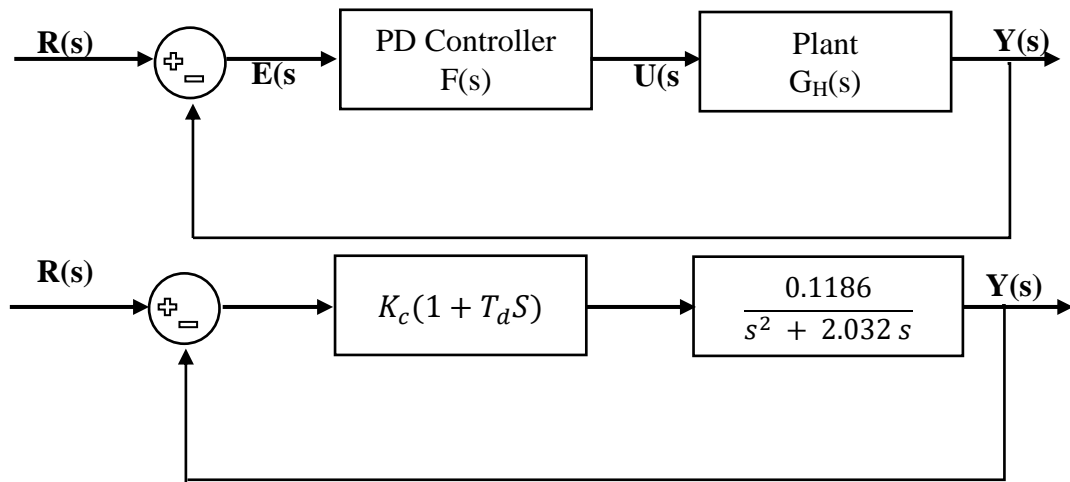


Figure 3.6 Closed-loop system block diagrams with a PD controller

In this work, we have designed a PD controller that satisfies 10% percentage overshoot and 3 seconds settling time with no steady state error. If some translations are applied, K_p and K_d can be find:

$$K_p = K_c \quad (3.3)$$

$$K_d = K_c \times T_d \quad (3.4)$$

3.4.2 Modelling Controller in LabVIEW

LABVIEW is the product of National Instruments, which is a powerful software system that fits the requirement for instrument control, data presentation, data acquisition, and data processing. It is a high-level programming language that follows the internal structures of the C language. It uses the G language (the graphical programming language) departing from the traditional high-level languages like Basic, Pascal or C language. However, it offers new simplicity and features regarding producing signal processing calculations. It can run on PC under many operating systems such as Windows, Linux, Apple Mac OSX, etc. The graphical program of LabVIEW known as Virtual Instruments or mainly VIs consists of Block Diagram and Front Panel. LabVIEW manages DAQ, analysis, and display into one system. To control instruments and to acquire data, the LabVIEW operates over RS-232, USB, and IEEE-488 (GPIB) protocols in addition to other A/D, D/A and digital I/O interface boards. LabVIEW analysis Library provides the user a wide-ranging of resources for linear algebra, statistical analysis, filtering, signal processing and many more. The LabVIEW from version 5 and up can support Active X Control making it possible for the user to control the object in Web Browser [22].

The LabVIEW toolkit assists to perfectly interface the NI-3635 DAQ with LabVIEW software. By used LabVIEW, we can control and acquire data from DAQ. In this work, we have designed a program that used to control the operation of a 1-DOF helicopter in both PID and SMC methods. It includes program structures that have the modeling and controller design, the graphical user interface (GUI) that utilized user in control operation and the real-time analysis viewport [27]. LabVIEW used in this thesis is a trial version.

3.4.3 Modelling Block Diagram

In this diagram, we have a model of the 1-DOF helicopter and input the dependence parameters. Figure 3.7 shows the system modeling for 1-DOF helicopter.

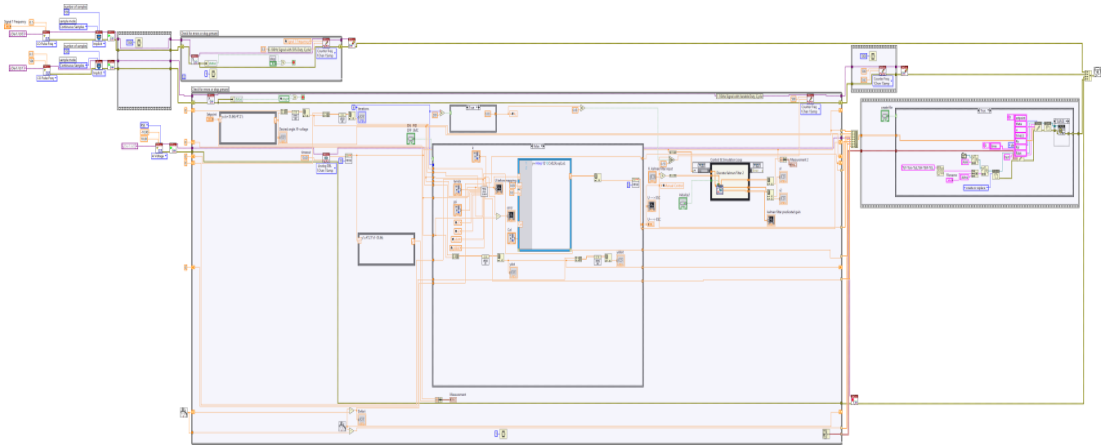


Figure 3.7 LabVIEW block diagram for modeling the 1-DOF helicopter

3.4.3.1 PID Block Diagram

In this diagram, we have designed the PID controller for 1-DOF helicopter Figure 3.8.

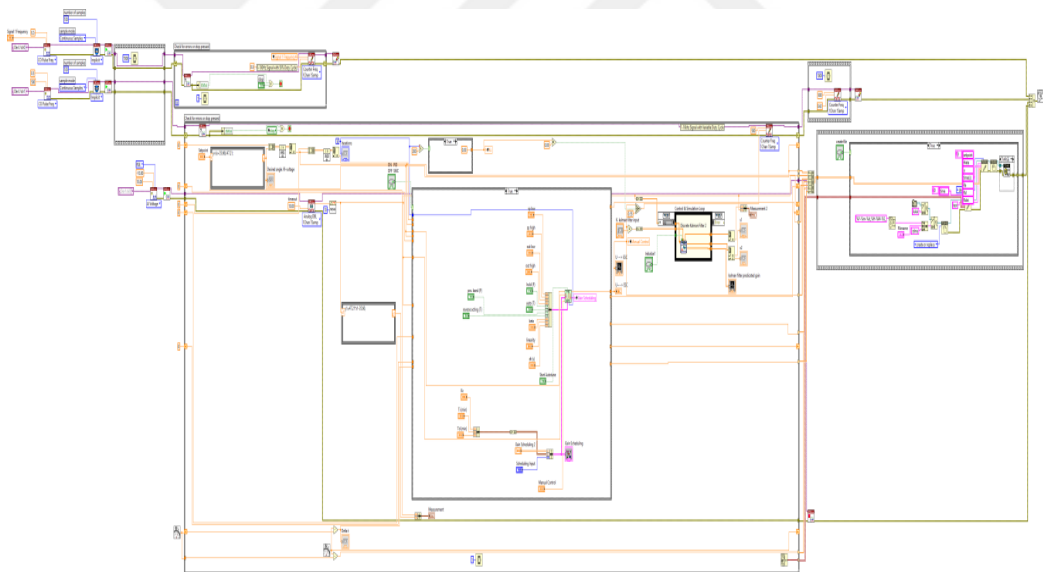


Figure 3.8 PID controller for 1-DOF helicopter in LabView (LabVIEW block diagram)

3.4.3.2 SMC Block Diagram

In this diagram, we have designed the SMC controller for 1-DOF helicopter Figure 3.9.

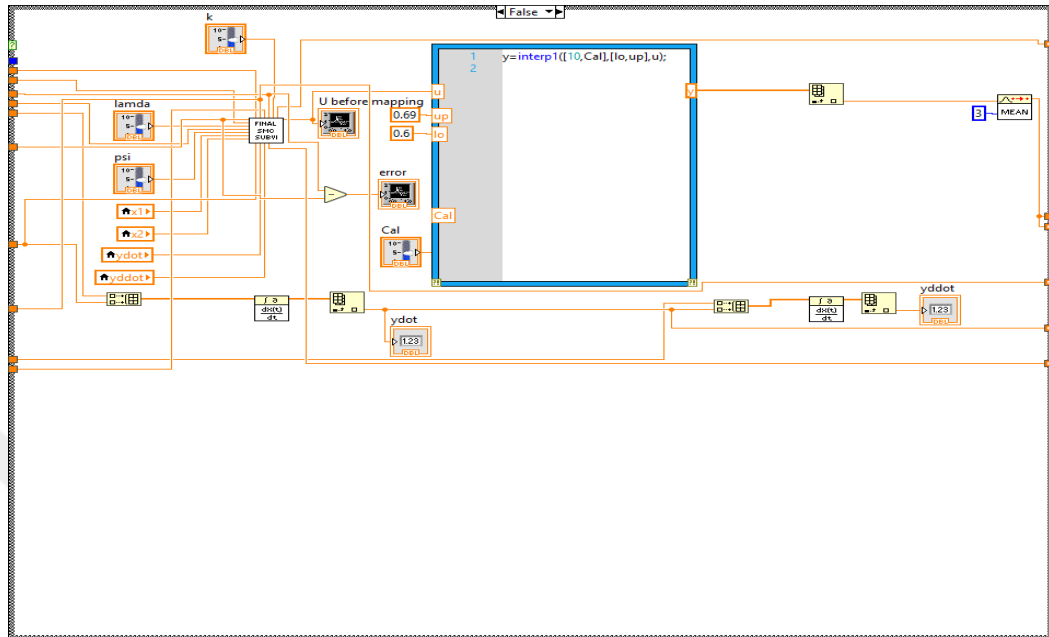


Figure 3.9 LabVIEW block diagram for the SMC controller of 1-DOF helicopter

3.4.3.3 Graphical User interface GUI

The GUI has been designed for easy control and monitoring the operation of 1-DOF helicopter as in Figure 3.10.

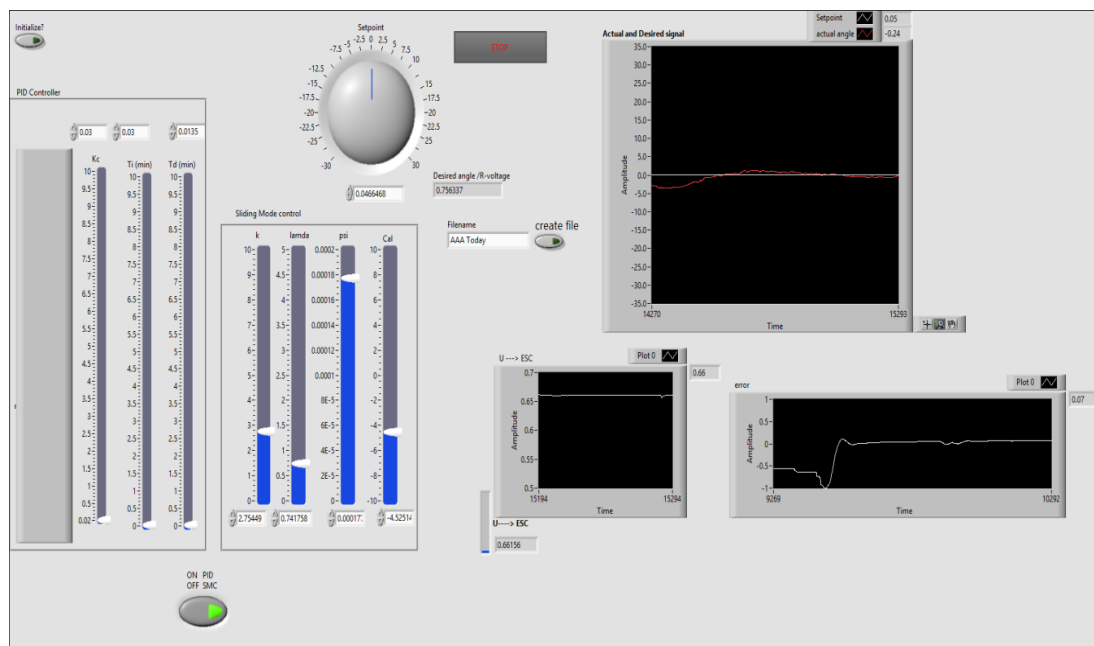


Figure 3.10 LabVIEW GUI for SMC controller for 1-DOF helicopter

It includes the following parameters: The output range bounds the output signal between two values and it forces the system to not exceed these boundary values, which are specified as output high and output low. Also there is a selection button for mode of operation to choose either PID or SMC, noticing that PID controller has addition input parameters like K_P , K_I , K_D .



CHAPTER FOUR

RESULTS AND DISCUSSION

This chapter shows the experimental results for the operation of 1-DOF helicopter and compares the results between the model that uses a PID controller with the model that utilizes the SMC controller.

4.1 Operation Results

This part tests the ability of the proposed helicopter to operate in 1-DOF by using PID and SMC, along with their response to change as a result to change in parameters in GUI. We first put the balancing weight in the center of the slide (default position) then power on the system. The controller then controls the voltage of motor that starts rotating the propeller and increases its speed until arm rises up and then modifying its value until it reaches the balancing mode. Figures 4.1 and 4.2 show the proposed system operation using PID, SMC and when both of them are off.



Figure 4.1 The mode selection and real-time monitoring from GUI for proposed 1-DOF helicopter

The operation results show that the proposed controller has successfully balanced the 1-DOF helicopter in both PID and SMC modes. Figure 4.2 shows the 1-DOF helicopter at balanced state.

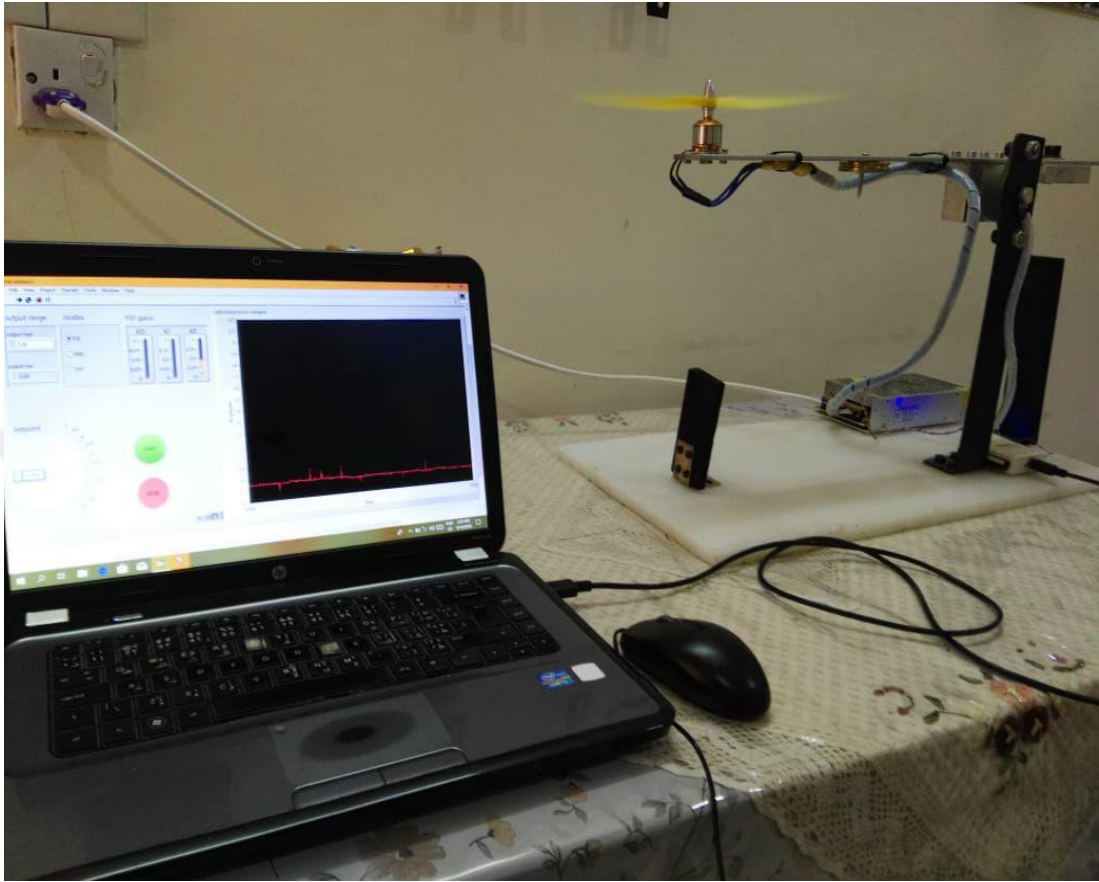


Figure 4.2 1-DOF helicopter balance through the operation

4.2 System Balance Results

This part tests the 1-DOF system balance of both PID and SMC, and then compares the results of both controllers to determine the practical way in 1-DOF control. In this test, we changed the balancing mass to investigate the ability of the proposed system to rebalance itself to stable mode and calculated the response time of both controller models.

4.3 PID controller:

Case one:

We have moved mass from the center of the slide to the slider's end that is inside of the motor, and then we have checked the processing variable (PV) results. Figure 4.3 shows the response time results for the PID controller.

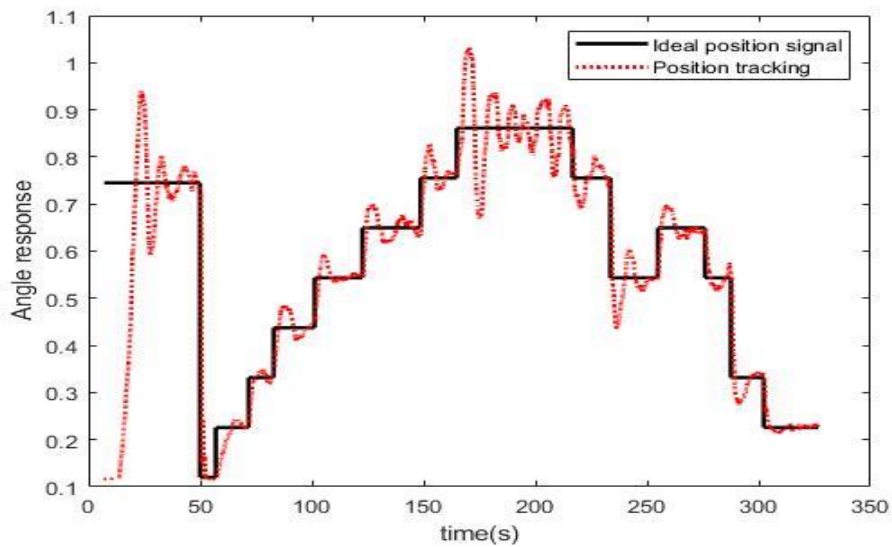


Figure 4.3 Tracking signal by using PID process variables of 1-DOF helicoptered when balancing mass moves to slider's end inside of the motor

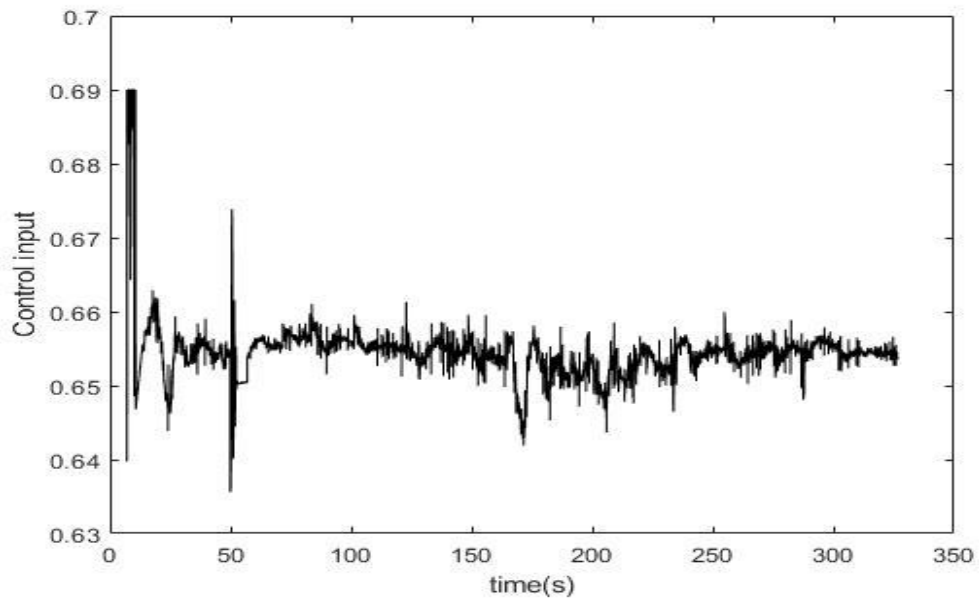


Figure 4.4 control input $u(t)$ by using PID process variables of 1-DOF helicoptered when balancing mass moves to slider's end inside of the motor

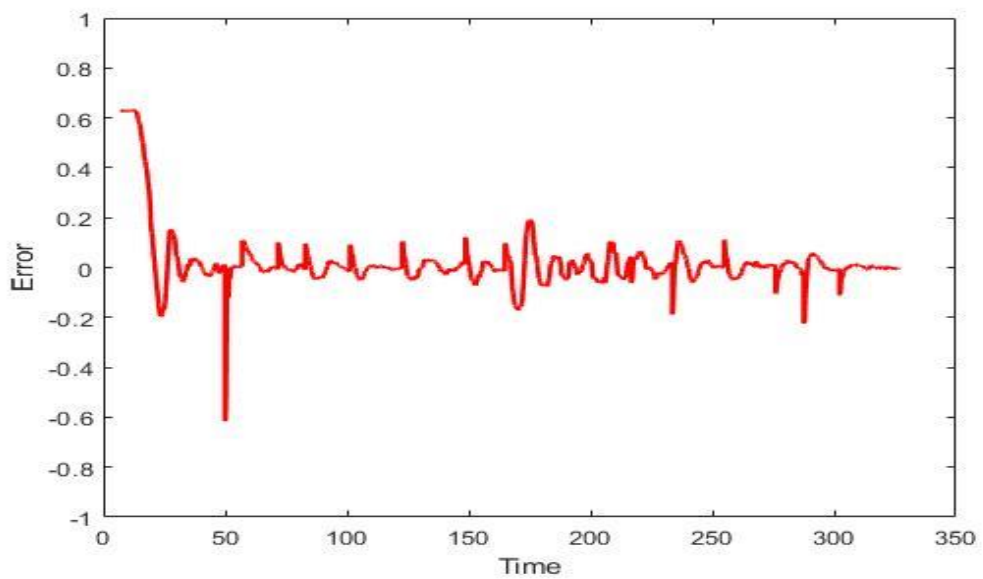


Figure 4.5 Error signal by using PID process variables of 1-DOF helicoptered when balancing mass moves to slider's end inside of the motor error signal

Case two:

We have moved balance mass from the center of the slide to slider's end that is inside of balancing block, then we have checked the processing variable (PV) results. Figure 4.6 shows the response time results for SMC.

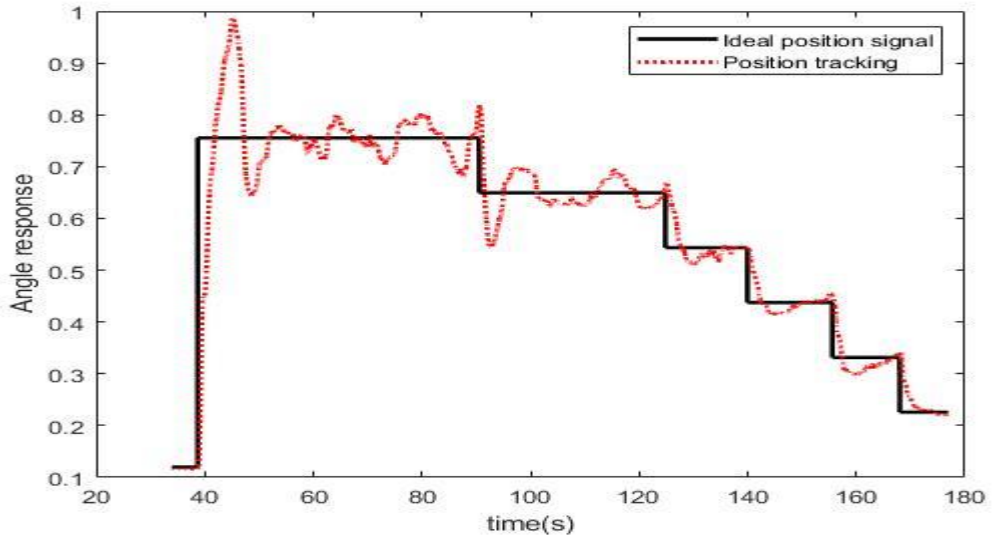


Figure 4.6 Tracking signal by using PID Process Variable of 1-DOF helicoptered when balancing mass moves to slider's end that is near balancing block.

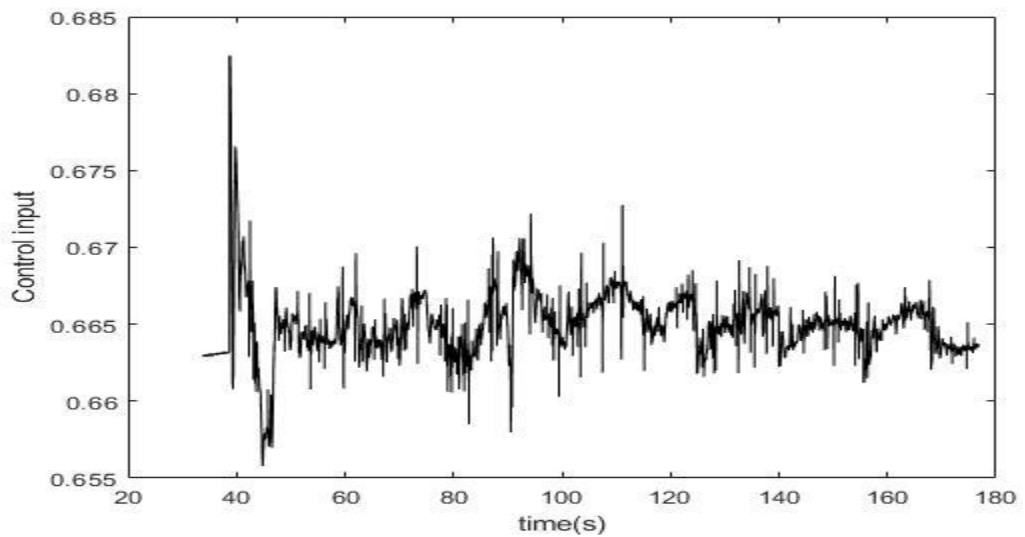


Figure 4.7 Control input $u(t)$ by using PID Process Variable of 1-DOF helicoptered when balancing mass moves to slider's end that is near balancing block.

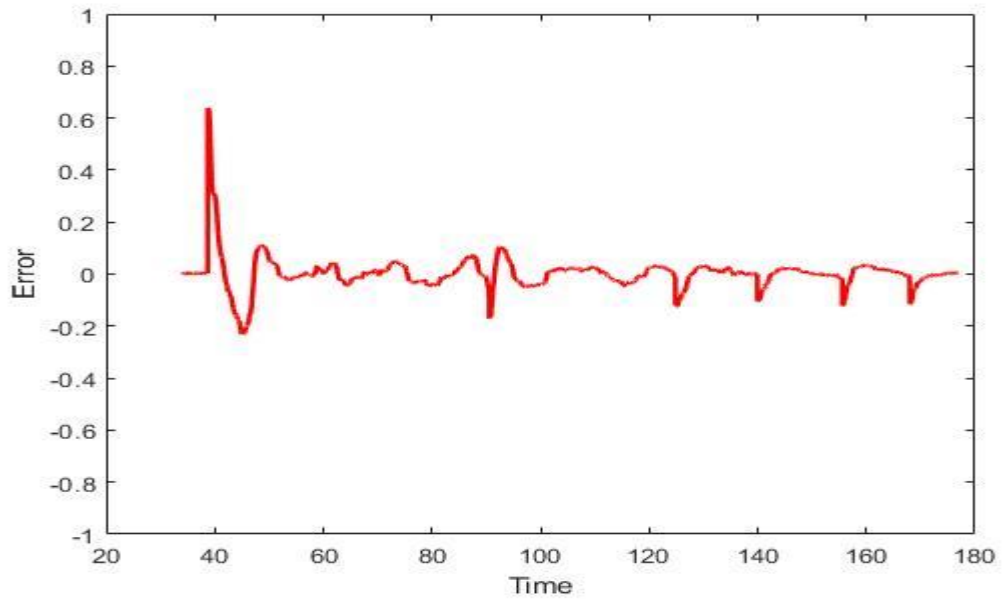


Figure 4.8 Error signal by using PID Process Variable of 1-DOF helicoptered when balancing mass moves to slider's end that is near the balancing block.

Case 3:

We have changed balance mass in the center of the slide, and then we have checked the tracking signal results. Figure 4.9 shows the response time.

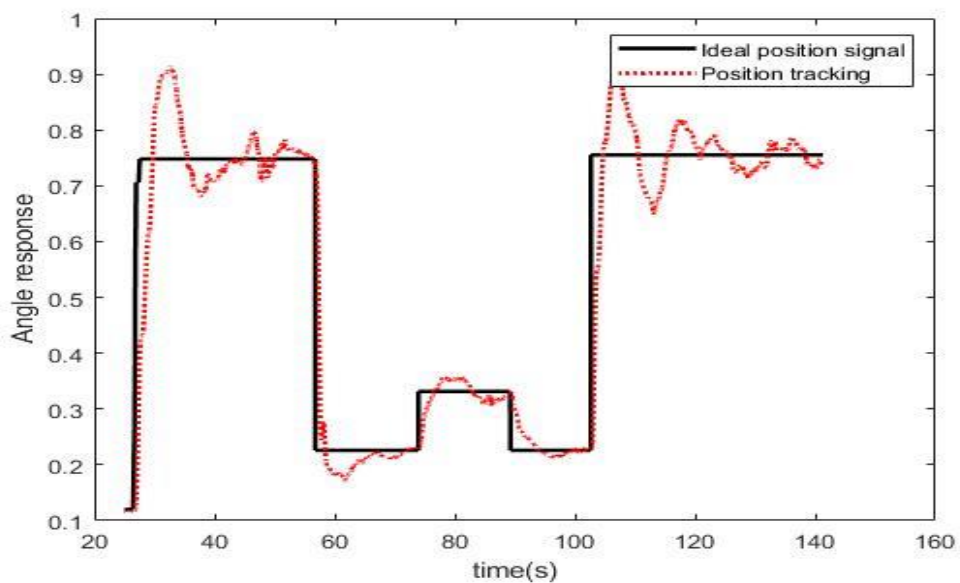


Figure 4.9 Tracking signal by using PID Process Variable of 1-DOF helicoptered when balancing mass changed to the center.

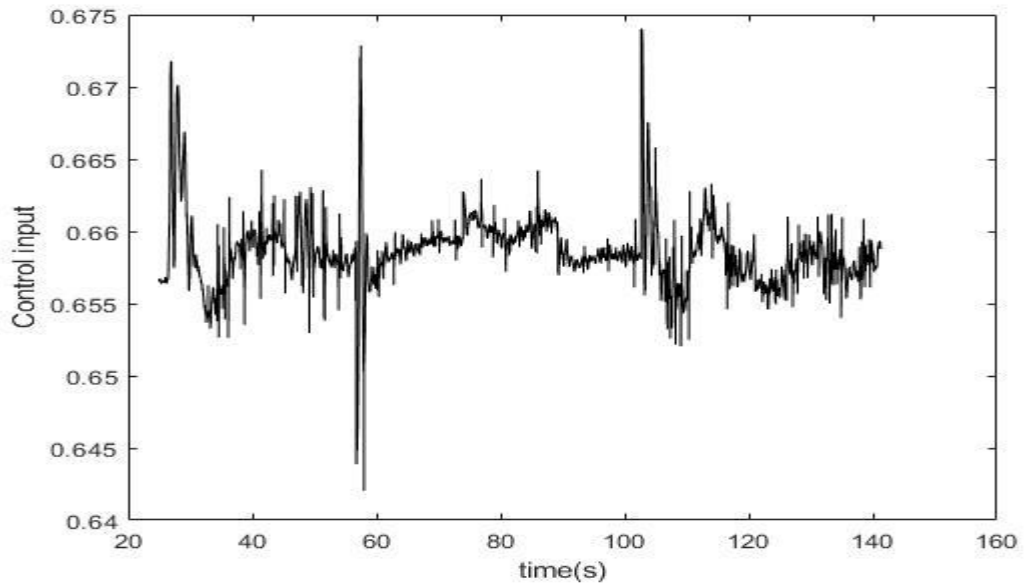


Figure 4.10 Control input $u(t)$ by using PID Process Variable of 1-DOF helicoptered when balancing mass changed to the center.

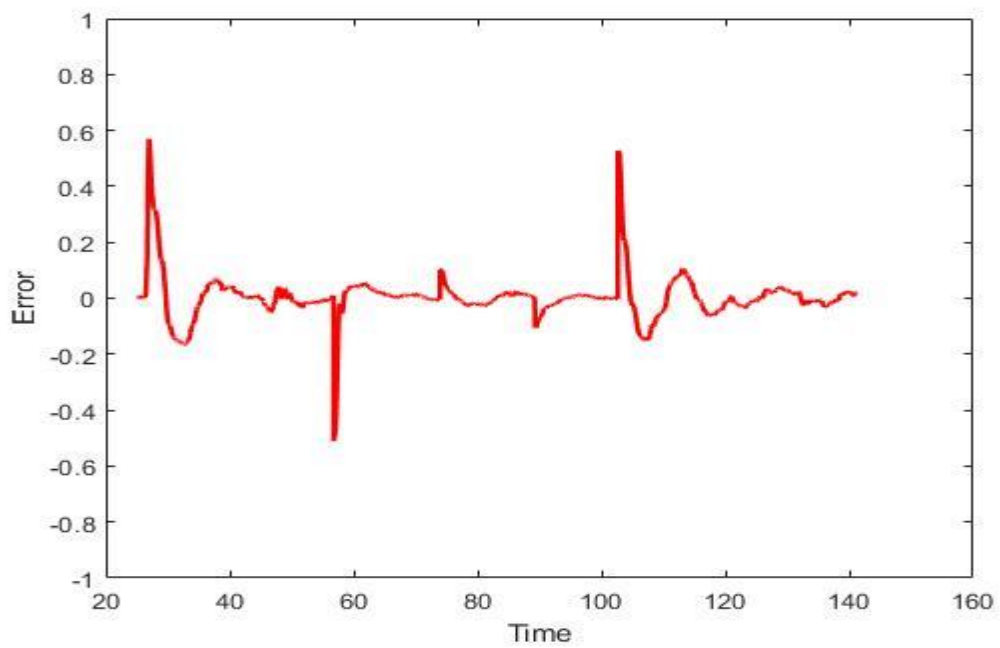


Figure 4.11 Error signal by using PID Process Variable of 1-DOF helicoptered when balancing mass changed to the center.

4.4 Sliding Mode controller

Case one:

We have put mass at the center of the slide, then we have checked the processing variable tracking signal. Figure 4.12 shows the response time results for SMC controller.

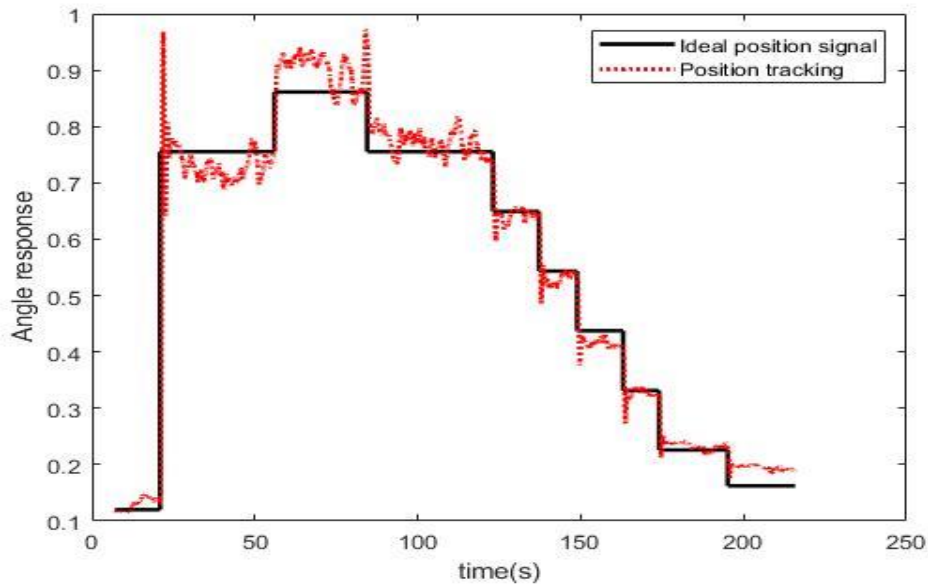


Figure 4.12 Tracking signal by SMC Process Variable of 1-DOF helicoptered when balancing mass centered at slider's at the side of the motor

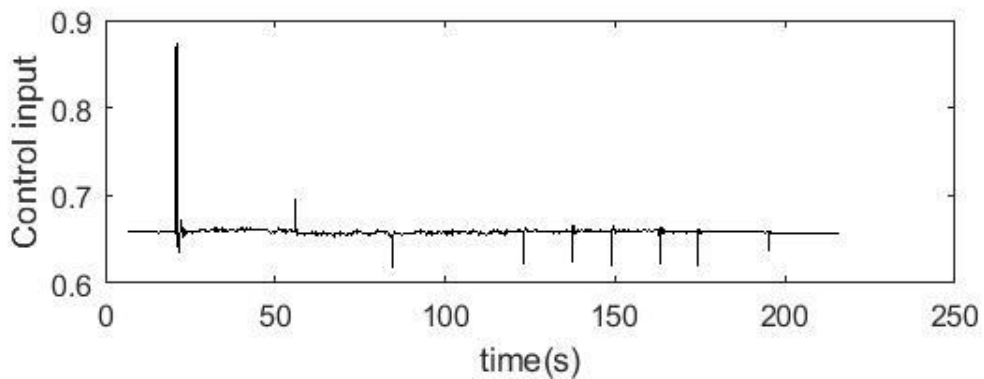


Figure 4.13 Control input $u(t)$ by SMC Process Variable of 1-DOF helicoptered when balancing mass centered at slider's at the side of the motor

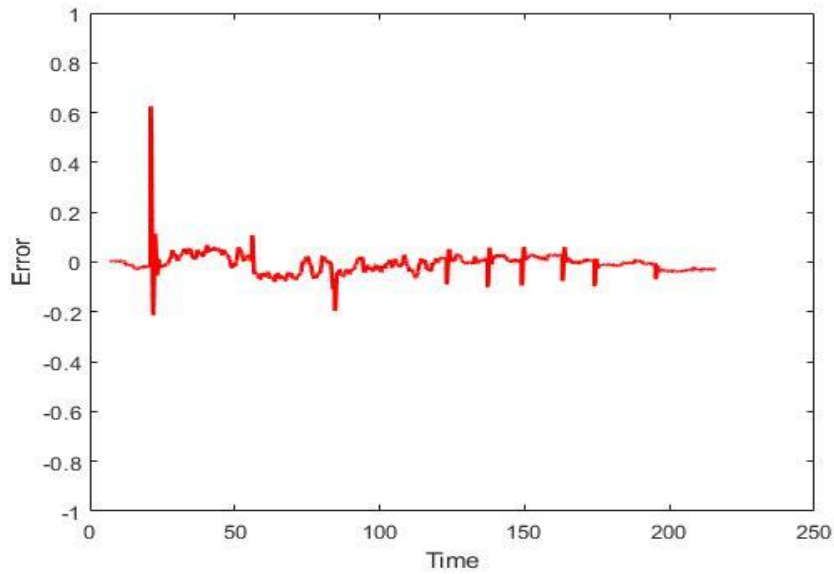


Figure 4.14 Error signal by SMC Process Variable of 1-DOF helicoptered when balancing mass centered at slider's at the side of the motor

Case two:

We have moved balance mass from the center of the slide to slider's end that is inside of balancing block, then we have checked the processing variable (PV) results. Figure 4.15 shows the response of the tracking signal and controlled input.

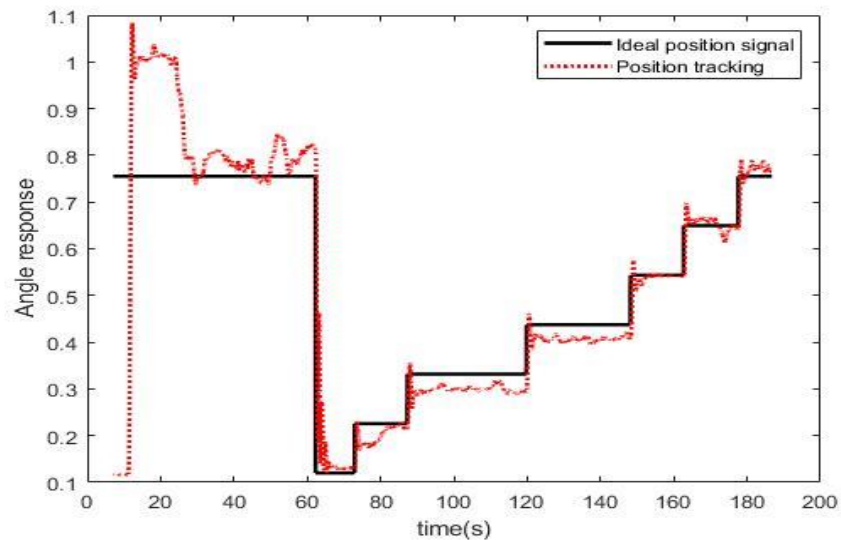


Figure 4.15 Tracking signal by SMC Process Variable of 1-DOF helicoptered when balancing mass moves to slider's end that is near balancing block

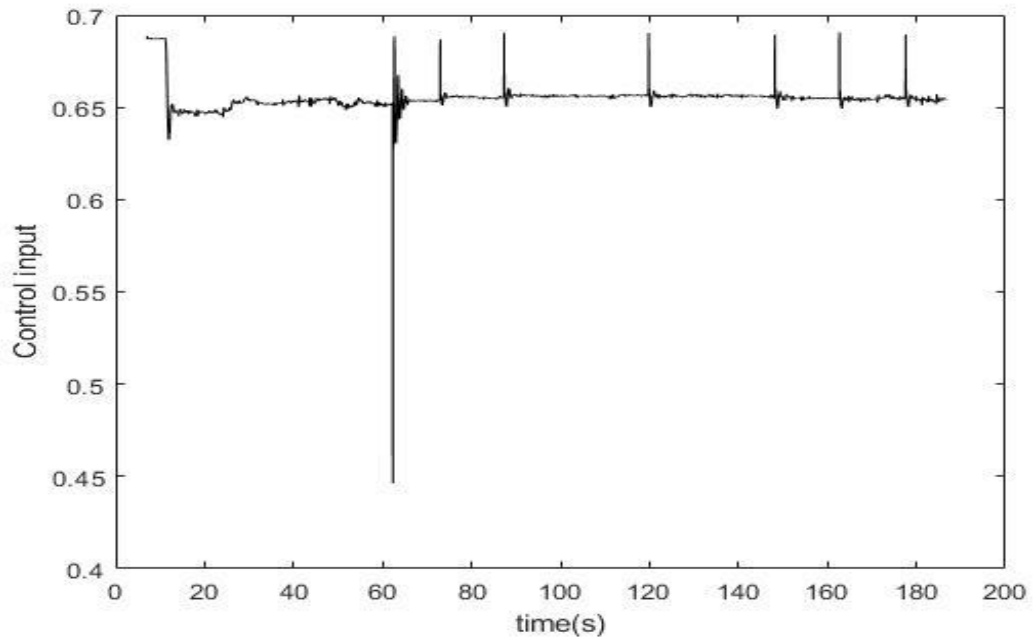


Figure 4.16 Control input $u(t)$ by SMC Process Variable of 1-DOF helicoptered when balancing mass moves to slider's end that is near balancing block

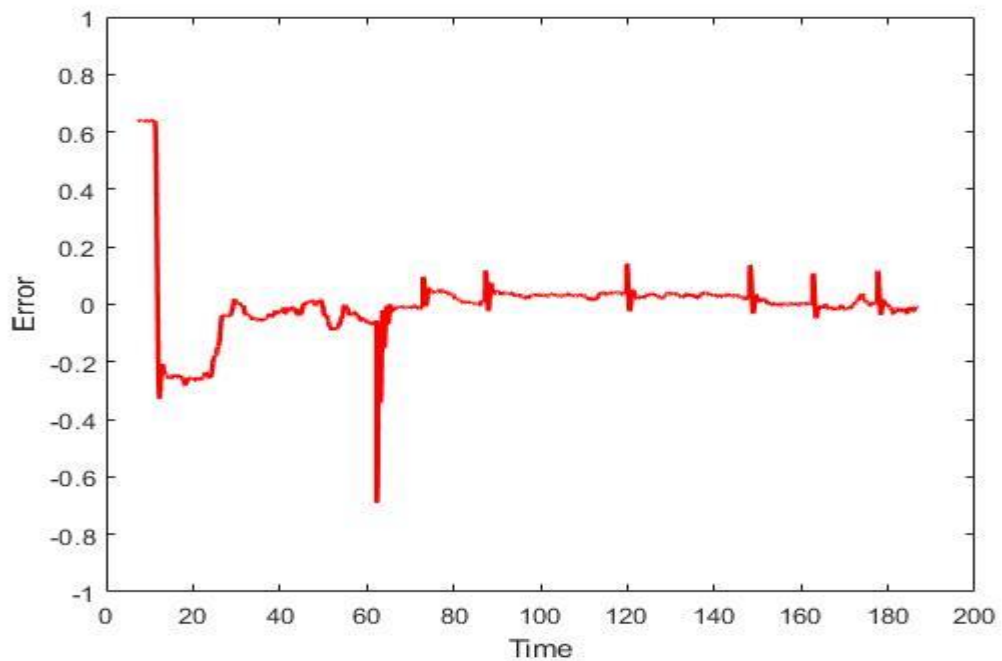


Figure 4.17 Error signal by SMC Process Variable of 1-DOF helicopter when balancing mass moves to slider's end that is near balancing block

Case 3:

We have changed balance mass in the center of the slide, then we have checked the tracking signal results. Figure 4.18 shows the response time

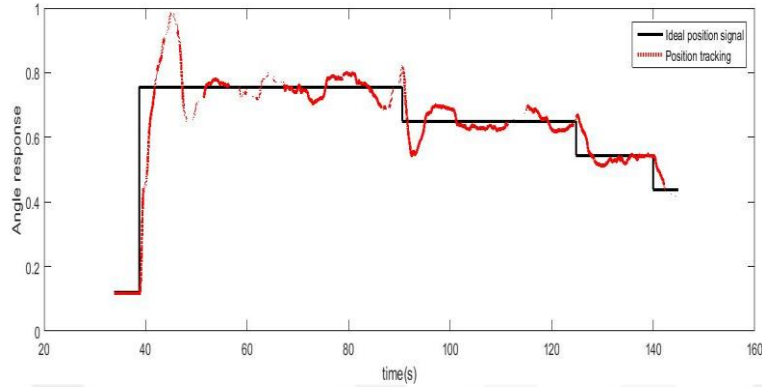


Figure 4.18 Tracking signal by SMC Process Variable of 1-DOF helicoptered when mass changed that located at the center of the motor side

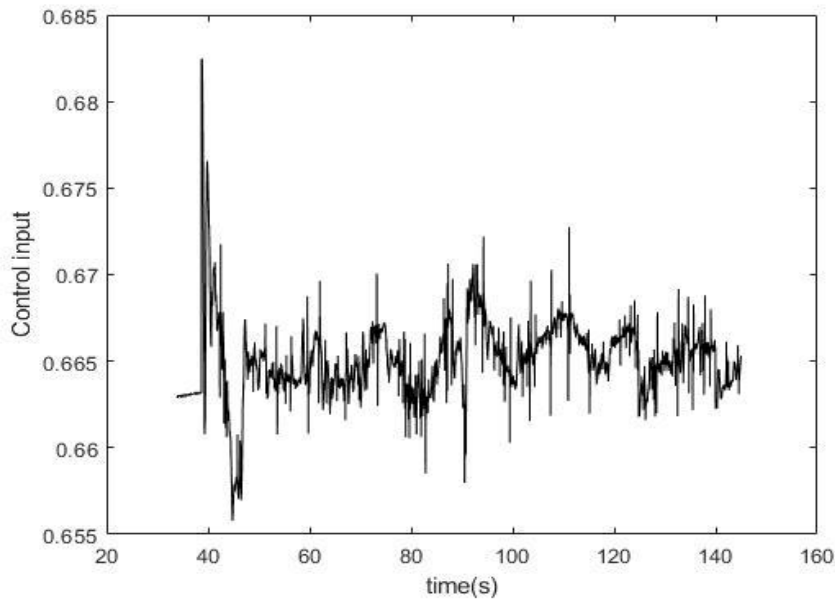


Figure 4.19 Control input by SMC Process Variable of 1-DOF helicoptered when mass changed that located at the center of the motor side

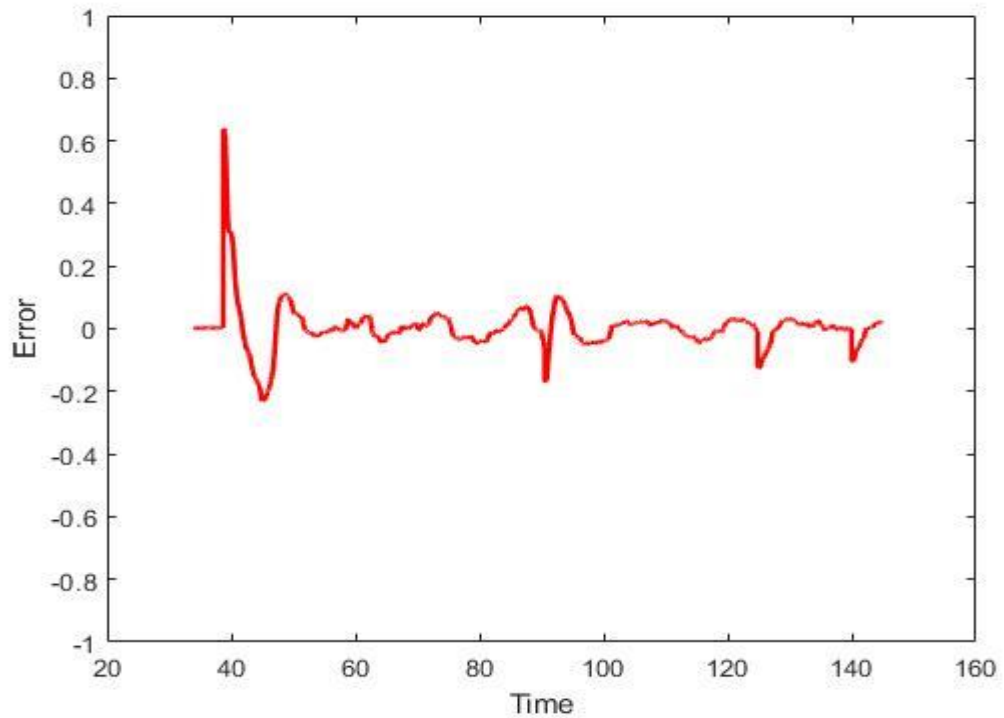


Figure 4.20 Error signal by SMC Process Variable of 1-DOF helicoptered when mass changed that located at the center of the motor side

Modern complex controllers often need more performance criteria than those presented so far. While the error and time are important factors and it should be considered simultaneously.

The performance index of Mean Square Error (MSE) is used to measure performance of both PID and SMC as shown in Table 4.1.

Table 4.1 Mean Square Error comparison of PID and SMC controllers

	MSE of PID	MSE of SMC
Nominal system	0.006500507	0.002873362
System with Δl disturbance	0.008366644	0.005532288
System with ΔM disturbance	0.015111378	0.001846474

Where Δl is the nominal mass is shifted from its position, ΔM is the nominal mass is changed at the same nominal location.

As shown from results in of PID and SMC, SMC has a faster response than PID which reach stability in case one in about in 4 seconds while PID takes about 13 seconds, for case two, SMC takes about 50ms while PID takes about 17 seconds, while the third case PID takes 15.5 seconds and SMC 13 seconds. In all studied cases, SMC is proved that its response is aster and it is a more reliable controller.



CHAPTER FIVE

CONCLUSIONS AND FUTURE WORKS

5.1 Conclusion

Designing an accurate DOF control system for controlling system balance play a significant role in a wide range of application such as robotics, autopilot, military application, aircraft, and similar. In this work, we have designed a control strategy for a 1-DOF helicopter model. We have investigated the use of two control systems using the PID controller and the SMC controller. The DAQ system from NI has been used for collecting feedback signal and actuating the hardware, and LabVIEW has been used to implement the controllers with a suitable GUI. Both controllers have been tested to determine the accuracy and performance. The results show that both controller models achieved balance for 1-DOF helicopter and they can keep the balance even with change of mass location along the arm. The test results show that the SMC is faster than the PID controller, whereas the PID can achieve 1-DOF balancing requirement in less complexity and better simplicity. The performance index of MSE has been used to reveal control performance of each controller and results show that SMC outperforms the PID in balancing the 1-DOF helicopter model specifically in presence of disturbances.

5.2 Future Works

Investigating the stability of proposed system in real flying conditions subject to environmental disturbances such as wind, rain can be studied as a future work. Observing and analysing the response and accuracy of both control strategies of SMC and PID under real circumstances can follow this research.

Investigating the use of PID and SMC in 2-DOF and 3-DOF problems and analysing performances can also be studies in the light of results presented in this thesis.

REFERENCES

- [1] Isidori, A., Marconi, L. , Serrani, A. (2003). Robust nonlinear motion control of a helicopter. *IEEE Transactions On Automatic Control*, **48**(3), 413-426.
- [2] Kondo, H., Ochi, Y., Sasano, S. (2011). PID controller design using fractional balanced reduction. In *SICE Annual Conference (SICE)*, 1791-1796.
- [3] Briod, A., Kornatowski, P., Zufferey, J. C., Floreano, D. (2014). A Collision-resilient Flying Robot. *Journal of Field Robotics*, **31**(4), 496-509.
- [4] Jimenez-Cano, A. E., Braga, J., Heredia, G., Ollero, A. (2015). Aerial manipulator for structure inspection by contact from the underside. In *Intelligent Robots and Systems (IROS), 2015 IEEE/RSJ International Conference on* , **3**, 1879-1884.
- [5] Jimenez-Cano, A. E., Martin, J., Heredia, G., Ollero, A., Cano, R. (2013). Control of an aerial robot with multi-link arm for assembly tasks. *International Conference on Robotics and Automation ICRA*, **5**, 4916-4921.
- [6] Ferenando, Liu. (2001). Experimental Results on smoothing sliding control of uncertain systems, *IEEE conference on decision and control*, **1**, 928-933.
- [7] Dumanay, A., Istanbulu, A., Demirtas, A. (2016). Comparison of PID and SMC Methods in DC Motor Speed Control, *IOSR Journal of Electrical and Electronics Engineering*, **11**(6), 10-16.
- [8] Shimada, A., Fujita, M. (2006). Takeoff and landing control using force sensor by electrically-powered helicopters. In *Advanced Motion Control, 2006. 9th IEEE International Workshop on*, 62-65.
- [9] Tomei, P. (1991). Adaptive PD controller for robot manipulators. *IEEE Transactions on Robotics and Automation*, **7**(4), 565-570.

- [10] Andreas, V. H. (2015). Model, Design and Control of a Quad-copter, master thesis, Norwegian University of Science and Technology, 1-5.
- [11] Nuno, E., Ortega, R., Barabanov, N., Basañez, L. (2008). A globally stable PD controller for bilateral teleoperators. *IEEE Transactions on Robotics*, **24**(3), 753-758.
- [12] Su, C. Y., Leung, T. P., Zhou, Q. J. (1992). Force/motion control of constrained robots using sliding mode. *IEEE Transactions on Automatic Control*, **37**(5), 668-672.
- [13] Dolinsky, K., Jadlovska, A. (2011). Application of results of experimental identification in control of laboratory helicopter model, *Advance in electrical and Electronical Engineering*, **7**, 157-166
- [14] Hok, M. (2013). Helicopter in virtual space, master thesis, Lulea University of Technology, space science and Technology, Department of space science, Kiruna.
- [15] Sira-Ramirez, H., Zribi, M., Ahmad, S. (1994). Dynamical sliding mode control approach for vertical flight regulation in helicopters. *IEE Proceedings-Control Theory and Applications*, **141**(1), 19-24
- [16] Kizmaz, H., Aksoy, S., Mühürçü, A. Sliding mode control of suspended pendulum, (2010). *Modern Electric power systems*, Wroclaw, Poland, 14.
- [17] Vilchis, J. A., Brogliato, B., Dzul, A., Lozano, R. (2003). Nonlinear modeling and control of helicopters, *Automatica*, **39**, 1583–1596.
- [18] Igarashi, K., Hazawa K., Shin, J., Fujiwara, D., Dilshan, F., Nonami, K. (2003). Autonomous small unmanned helicopter Height and Automatic taking off and landing control, *Dynamics and Design Conference*, **8**, 91–95.
- [19] John J. (1981). Hybrid position/force control of manipulators. *Journal of Dynamic Systems, Measurement, and Control*, **103**, 2, 126–133.
- [20] Butt, Y. A., Bhatti, A. I. (2012). Robust altitude tracking of a helicopter using sliding mode control structure. In *Emerging Technologies (ICET), 2012 International Conference on*, **1**, 82.

- [21] Fumagalli, M., Carloni, R. (2013). A modified impedance control for physical interaction of UAVs. In Proc. of *2013 IEEE/RSJ International Conference on Intelligent Robots and Systems*, 1979–1984.
- [22] Chachou, M. Y., Liu, Z., Zhou, Z., Benchalal, A., Zerfaoui, C. (2014). Modeling, and Control of a Simulated Flight of a Mini Helicopter Using Matlab/Simulink. *The international conference on computer, communication and information technology*, **1**, 216-226
- [23] Hovakimyan, N., Nardi, F., Calise, A., Kim, N. (2002). Adaptive output feedback control of uncertain nonlinear systems using single-hidden layer neural networks, *IEEE Transactions on Neural Networks*, **13**(6), 1420–1431.
- [24] Nonami, K. (2007). Prospect and recent research & development for civil use autonomous unmanned aircraft as UAV and MAV. *Journal of system Design and Dynamics*, **1**(2), 120-128.
- [25] Nikhil, et. al. (2012). Control of multiple UAVs for persistent surveillance: algorithm and flight test results, *IEEE Transactions on Control Systems Technology*, **20**(5), 1236–1251,.
- [26] Enns, R., Si, J. (2003). Helicopter trimming and tracking control using direct neural dynamic programming. *IEEE Trans. Neural Netw*, **14**(4), 929–939.
- [27] Chuei, R., Cao, Z., Man, Z. (2016). Sliding Mode based Repetitive Control for Parameter Uncertainty of a Brushless DC Servo Motor. *International Conference on Advanced mechatronic systems*, **1**, 62-67.
- [28] Devasia, S. (1997). Output tracking with nonhyperbolic and near on hyperbolic internal dynamics Helicopter hover control. *Journal and Guidance, Control and Dynamics*, **20**(3), 573–580.
- [29] Norouzi Ghazbi, S., Aghli, Y., Alimohammadi, M., Akbari, A. (2016). Quadrotors Unmanned Aerial Vehicles: A Review, *International Journal On Smart Sensing And Intelligent Systems*, **9**(1), 309–333.
- [30] Nilsen, N. (2017). Modeling and Control of Two Degrees of Freedom Helicopter Model, master thesis, The University College of Southeast Norway.

- [31] Koo, T. K. J., Sastry, S. S. (1998). Output tracking control design of a helicopter model based on approximate linearization, in *Proc. 37th IEEE Conference Decision Control*, **2**, 3635–3640.
- [32] Tsuchiya, Y., Yashiro, D., Yubai, K., Komada, S. (2017). Contact force control of a dual-rotor helicopter with protect the frame. In *Industrial Technology (ICIT), 2017 IEEE International Conference on* , **1**, 659-664.
- [33] Salazar, T. (2010). Mathematical model and simulation for a helicopter with a tail rotor. *Advances in computational intelligence-man machine system and cybernetics*, **1**, 27-33.
- [34] William S., the control handbook, 2nd edition. CRC press.
- [35] www.ni.com/en-tr/support/documentation/product-certifications/model.usb-6353.html [accessed 03.08.2018].